

The marine n-3 PUFA DHA evokes cytoprotection against oxidative stress and protein misfolding by inducing autophagy and NFE2L2 in human retinal pigment epithelial cells

Ida Johansson,^{1,2,3} Vivi Talstad Monsen,¹ Kristine Pettersen,^{1,2,3} Jennifer Mildenerger,^{2,3,4} Kristine Misund,^{4,5} Kai Kaarniranta,^{6,7} Svanhild Schönberg,¹ and Geir Bjørkøy^{2,3,*}

¹Department of Laboratory Medicine; Children's and Women's Health; Faculty of Medicine; Norwegian University of Science and Technology; Trondheim, Norway; ²Department of Technology; University College of Sør-Trøndelag; Trondheim, Norway; ³Centre of Molecular Inflammation Research and Department of Cancer Research and Molecular Medicine; Norwegian University of Science and Technology; Trondheim, Norway; ⁴Department of Cancer Research and Molecular Medicine; Faculty of Medicine; Norwegian University of Science and Technology; Trondheim, Norway; ⁵KG Jebsen Center for Myeloma Research; Norwegian University of Science and Technology; Trondheim, Norway; ⁶Department of Ophthalmology; Institute of Clinical Medicine; University of Eastern Finland; Kuopio, Finland; ⁷Department of Ophthalmology; Kuopio University Hospital; Kuopio, Finland

Keywords: AA, antioxidants, autophagy, DHA, HMOX1, LC3B, MAP1LC3B, NFE2L2, NRF2, OA, omega-3, p62, PUFA, ROS, SQSTM1

Abbreviations: AA, arachidonic acid; AMD, age-related macular degeneration; AREDS, Age-Related Eye Disease Study; ATF4, activating transcription factor 4; ATG4, autophagy-related 4; BafA1, bafilomycin A₁; CHX, cycloheximide; CREB, cAMP responsive element binding protein; DCF, 5-(and-6)-carboxy-2',7'-dichlorodihydrofluorescein diacetate; DHA, docosahexaenoic acid; ER, endoplasmic reticulum; HMOX1, heme oxygenase 1; KEAP1, kelch-like ECH-associated protein 1; MAP1LC3B, microtubule-associated protein 1 light chain 3 β; MEF, mouse embryonic fibroblast; NAC, N-acetyl cysteine; NQO1, NAD(P)H dehydrogenase, quinone 1; NFE2L2, nuclear factor, erythroid derived 2, like 2; OA, Oleic acid; POS, photoreceptor outer segment; PPARα, peroxisome proliferator-activated receptor α; PUFA, polyunsaturated fatty acid; qRT-PCR, quantitative real-time polymerase chain reaction; ROS, reactive oxygen species; RPE, retinal pigment epithelial; SLC7A11, solute carrier family 7 (anionic amino acid transporter light chain, xc- system), member 11; SRXN1, sulfiredoxin 1; SQSTM1, sequestosome 1; TFEB, transcription factor EB; UBA, ubiquitin associated domain; WT, wild type.

Accumulation and aggregation of misfolded proteins is a hallmark of several diseases collectively known as proteinopathies. Autophagy has a cytoprotective role in diseases associated with protein aggregates. Age-related macular degeneration (AMD) is the most common neurodegenerative eye disease that evokes blindness in elderly. AMD is characterized by degeneration of retinal pigment epithelial (RPE) cells and leads to loss of photoreceptor cells and central vision. The initial phase associates with accumulation of intracellular lipofuscin and extracellular deposits called drusen. Epidemiological studies have suggested an inverse correlation between dietary intake of marine n-3 polyunsaturated fatty acids (PUFAs) and the risk of developing neurodegenerative diseases, including AMD. However, the disease-preventive mechanism(s) mobilized by n-3 PUFAs is not completely understood. In human retinal pigment epithelial cells we find that physiologically relevant doses of the n-3 PUFA docosahexaenoic acid (DHA) induce a transient increase in cellular reactive oxygen species (ROS) levels that activates the oxidative stress response regulator NFE2L2/NRF2 (nuclear factor, erythroid derived 2, like 2). Simultaneously, there is a transient increase in intracellular protein aggregates containing SQSTM1/p62 (sequestosome 1) and an increase in autophagy. Pretreatment with DHA rescues the cells from cell cycle arrest induced by misfolded proteins or oxidative stress. Cells with a downregulated oxidative stress response, or autophagy, respond with reduced cell growth and survival after DHA supplementation. These results suggest that DHA both induces endogenous antioxidants and mobilizes selective autophagy of misfolded proteins. Both mechanisms could be relevant to reduce the risk of developing aggregate-associate diseases such as AMD.

© Ida Johansson, Vivi Talstad Monsen, Kristine Pettersen, Jennifer Mildenerger, Kristine Misund, Kai Kaarniranta, Svanhild Schönberg, and Geir Bjørkøy

*Correspondence to: Geir Bjørkøy; Email: geir.bjorkoy@hist.no

Submitted: 10/07/2014; Revised: 06/02/2015; Accepted: 06/05/2015

<http://dx.doi.org/10.1080/15548627.2015.1061170>

This is an Open Access article distributed under the terms of the Creative Commons Attribution-Non-Commercial License (<http://creativecommons.org/licenses/by-nc/3.0/>), which permits unrestricted non-commercial use, distribution, and reproduction in any medium, provided the original work is properly cited. The moral rights of the named author(s) have been asserted.

Introduction

Damaged proteins may have deleterious effects on cellular functions, and accumulation of misfolded proteins is the hallmark of several neurodegenerative diseases such as Huntington, Parkinson, and Alzheimer diseases and other age-related disorders.¹⁻⁶ Age-related macular degeneration (AMD) is a neurodegenerative disease of the eye and the leading cause of central blindness in western countries.^{7,8} Currently, for 80% to 85% of the 30 to 50 million AMD patients worldwide there are no effective treatment alternatives.⁹ Therefore, one major public health challenge is to devise an effective primary prevention of AMD and to improve current treatments.

The pathogenesis of AMD is initiated by degeneration and death of retinal pigment epithelial (RPE) cells followed by loss of the overlying photoreceptor neurons rod and cones.¹⁰ Increased accumulation of intracellular auto-oxidative and autofluorescent lipofuscin in the lysosomes of RPE cells, as well as drusen formation in the extracellular space between the RPE and the Bruch membrane are hallmarks of AMD.^{8,11-13} Lipofuscin is a brown-yellow, electron-dense, age-related pigment composed of a complex heterogeneous mixture of lipid-protein aggregates.¹⁴ In drusen various acute phase inflammatory markers and oxidative stress-related proteins have been characterized.¹⁵⁻¹⁷ Oxidative processes have been proposed to play a contributing role in AMD. RPE cells are exposed to chronic oxidative stress due to constant exposure to sunlight and relatively high oxygen tension, and high concentration of lipid peroxidation products from the ingested photoreceptor outer segments (POS).^{10,18,19} Oxidatively damaged proteins post-translationally modified e.g. with carboxyethylpyrrole, malondialdehyde, 4-hydroxynonenal, and advanced glycation end products, accumulate in the macular area and serve to further elevate oxidative stress.²⁰ It is unclear whether accumulation and aggregation is the cause or the consequence of the disease. However, high amounts of deposits predict AMD progression and severity and it is thought that this aggregation of misfolded proteins occurs after failure of the cellular protein quality control mechanisms of the cells.²¹ However, the role of aggregates in pathologies is controversial and may even protect the cells by sequestering putatively harmful soluble misfolded proteins. In Huntington disease it has been suggested that formation of aggregates may serve a cytoprotective role.²² In addition, aggregates may also facilitate the clearance of the toxic materials.²¹

Two major proteolytic systems are responsible for maintaining the cellular function: the proteosomal and lysosomal system. Both systems remove irreversibly damaged proteins and recycle amino acids for protein synthesis. The activity of these systems decline upon aging.²³ Macroautophagy (hereafter referred to as autophagy) is a catabolic process that removes damaged and foreign intracellular components by lysosomal degradation.²⁴ During autophagy, targeted cytoplasmic proteins and organelles are sequestered by a growing double membrane that forms an autophagosomal vesicle where the content is degraded after fusion with a lysosome. The rate of cellular turnover by autophagy increases in response to cellular stresses like starvation,

endoplasmic reticulum (ER) stress, and elevated levels of reactive oxygen species (ROS) for maintenance of cellular homeostasis.²⁵⁻²⁷ The SQSTM1/p62 protein (hereafter referred to as SQSTM1) binds both to ubiquitinated cargos, such as misfolded proteins and protein aggregates via its ubiquitin-associated (UBA) domain and also to the mammalian orthologs of yeast Atg8, located on the phagophore membrane.²⁸ In this way, SQSTM1 selectively targets ubiquitinated protein aggregates to lysosomal degradation.^{28,29} A specific binding of SQSTM1 to misfolded and ubiquitinated proteins, and its presence in cytoplasmic inclusions in diverse human diseases have suggested a general role of SQSTM1 in diseases associated with protein aggregates.⁵

Tissue-specific knockout of autophagy genes in neurons or hepatocytes results in early onset neurodegeneration and liver failure, respectively, accompanied by accumulation of misfolded protein aggregates and ubiquitinated proteins.^{30,31} Inducible knockout of autophagy in mice limits survival to 2 to 3 mo due to development of severe neurodegeneration.³² These findings suggest that autophagy is an important cytoprotective mechanism that counteracts the development of several age-related diseases, especially proteinopathies, by clearance of damaged proteins and organelles.³³ Lysosomal-mediated clearance is also important in RPE cells³⁴ supporting the idea that also in RPE cells, autophagy is critical to maintain cellular homeostasis. Whether autophagy could be induced as a disease preventive mechanism in these cells is still uncertain. However, caloric restriction and compounds like resveratrol can extend life span in different model organisms possibly due to increased autophagy.^{35,36}

Epidemiological studies indicate an inverse correlation between dietary intake of fish and the risk of developing AMD.³⁷⁻⁴² The disease preventive effects of increased fish intake have been associated with the content of marine omega-3 polyunsaturated fatty acids (n-3 PUFAs).⁴³ Deficiency of n-3 PUFAs in photoreceptors is associated with the development of AMD.⁴⁴ Increased intake of marine n-3 PUFAs has also been suggested to reduce the risk of other age-related disorders such as neurodegenerative diseases, different types of cancer, and heart and circulatory diseases.⁴⁵⁻⁴⁷ However, the disease preventive mechanism(s) mobilized by dietary n-3 PUFAs are not completely understood. Previously, several reports have suggested a change in autophagy in cancer cell lines that are sensitive and display cytotoxic and/or cytostatic responses to physiological doses of PUFAs.⁴⁸⁻⁵³ We explore whether increased autophagy is a part of the cellular response to PUFAs also in spontaneously arising ARPE-19 cells. If so, we hypothesize a correlation between the disease preventive effects of n-3 PUFAs and stimulation of autophagy in retinal pigment epithelial cells where the initial phases of AMD occurs.

Here we report that the n-3 PUFA docosahexaenoic acid (DHA, 22:6, n-3), in contrast to the n-6 PUFA arachidonic acid (AA, 20:4, n-6) and the n-9 fatty acid oleic acid (OA, 18:1, n-9), induces a transient increase in reactive oxygen species (ROS) in spontaneously arising retinal pigment epithelial cells. This mild, subtoxic stress is counteracted by activation of the antioxidant stress response transcription factor NFE2L2/NRF2 (nuclear factor, erythroid derived 2, like 2) that controls the transcription of

a number of genes encoding endogenous enzymatic and nonenzymatic antioxidants. DHA also causes a selective rise in SQSTM1 mRNA and protein levels in an NFE2L2-dependent manner. Further we observe a transient increase in sequestration of misfolded proteins into aggregates after DHA that coincides with an increase in autophagy that could facilitate clearance of the protein aggregates. In line with a mobilization of a protective response, we find that DHA increases the tolerance for oxidative stress and misfolded proteins in retinal pigment epithelial cells.

Results

The n-3 PUFA DHA induces protein aggregation and autophagy in ARPE-19 cells

n-3 PUFAs have been suggested to mobilize disease preventive effects for several age-related diseases. Since insufficient autophagy has been proposed to contribute in the development of several of the same diseases, we asked if n-3 PUFA supplementation could induce autophagy. Cellular responses to lipids were determined in the presence of serum to mimic the in vivo situation. The n-3 PUFA DHA (22:6, n-3) was used in final concentrations of 70 μ M and 140 μ M in the cell culture experiments which is well within physiological relevant levels found in serum of healthy individuals.⁵⁴ The diploid, spontaneously derived ARPE-19 human retinal pigment epithelial cells⁵⁵ were used as a model system since these cells are relevant for the development of AMD. To determine the basal autophagy flux in these cells, cell extracts were analyzed by immunoblot for accumulation of lipidated microtubule-associated protein 1 light chain 3 β (MAP1LC3B-II/LC3B-II) and SQSTM1 in the absence or presence of the autophagy/lysosomal inhibitor bafilomycin A₁ (BafA1) for different time points. In exponentially growing ARPE-19 cells, both SQSTM1 and MAP1LC3B-II protein levels displayed a linear increase with time throughout the experiment. The doubling time for

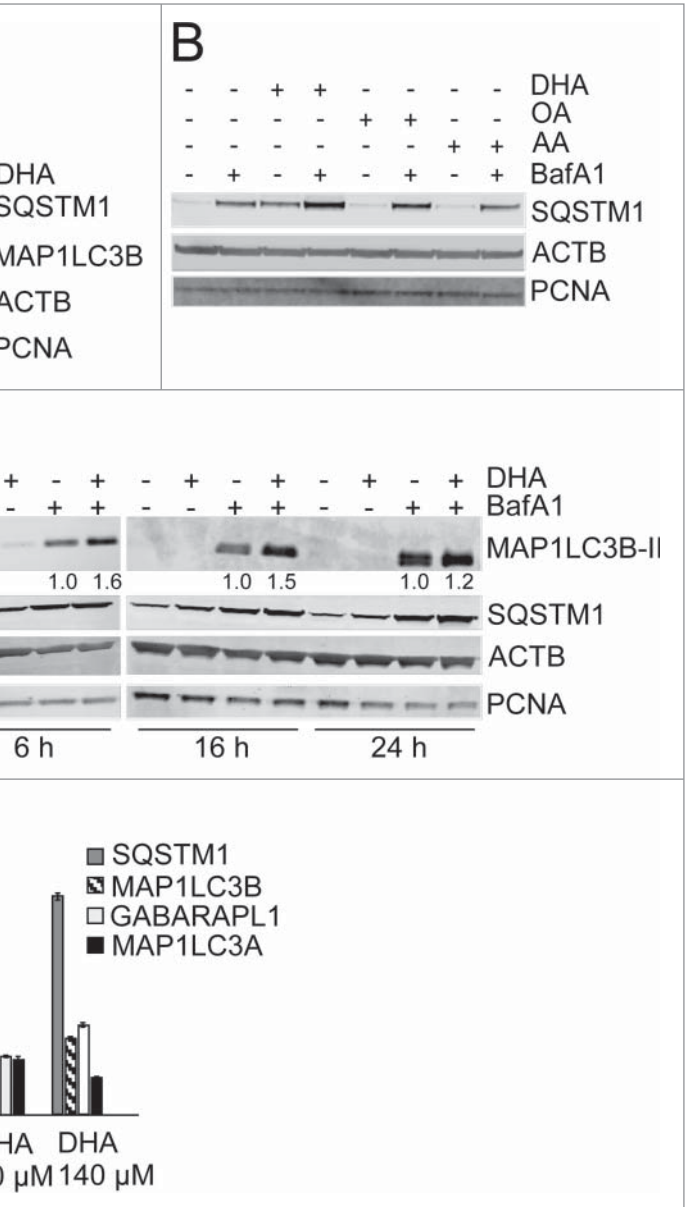


Figure 1. The n-3 PUFA DHA increases protein level of SQSTM1 and induces autophagy in ARPE-19 cells. **(A)** Cells were treated with DHA (70 μ M) for 24 h and lysed in Triton X-100 (Tx100) buffer. Equal amounts of protein (20 μ g) from T \times 100 fraction were centrifugated at 10,000 \times g and the pellet was dissolved in the same volume of 8 M urea buffer before loading on the gel. The membrane was immunoblotted for SQSTM1 and MAP1LC3B. β -actin (ACTB) and PCNA are used as loading controls. **(B)** The cells were treated with DHA, OA or AA (70 μ M) with or without BafA1 (100 nM) for 16 h. Total cell extracts were immunoblotted for SQSTM1. ACTB and PCNA are used as loading controls. **(C)** Protein levels of SQSTM1 and MAP1LC3B determined by immunoblotting of cells treated with DHA (70 μ M), BafA1 (100 nM) or a combination of DHA and BafA1 for the indicated time points. The numbers below the MAP1LC3B-II bands represent fold change relative to BafA1 for each time point normalized to PCNA intensity. ACTB and PCNA are used as loading controls. **(D)** The mRNA levels of *SQSTM1*, *MAP1LC3B*, *MAP1LC3A*, and *GABARAPL1* relative to *ACTB* after DHA (70 and 140 μ M) supplementation for 16 h determined by quantitative real-time PCR. qRT-PCR data displayed are representative for 2 independent experiments. Mean fold change from triplicate wells \pm SD is displayed. Data shown are representative of 3 or more independent experiments, unless otherwise stated.

SQSTM1 and MAP1LC3B-II was determined to be approximately 7 h and 5 h, respectively (Fig. S1). Since SQSTM1 is associated with protein aggregates that might be resistant to

detergents, the pellets that remain after Triton X-100 protein extraction and centrifugation of the lysates, were resolved in a buffer containing 8 M urea to also solubilize detergent-resistant proteins. A very clear increase in SQSTM1 protein level was observed in response to DHA in the detergent-resistant pellet while very little MAP1LC3B could be detected (Fig. 1A). During the rest of the study, cells were lysed directly in a buffer containing 8 M urea to avoid losing part of the cellular pool of SQSTM1. We then tested whether other lipids also could induce the level of SQSTM1. Interestingly, whereas stimulation with DHA clearly increased the protein level of SQSTM1, that was further elevated when combining DHA and BafA1 (Fig. 1B), no increase was observed after treatment with OA nor AA (Fig. 1B). The SQSTM1 gene is induced in response to different types of cellular stresses and the protein is continuously turned over by autophagy. Since combining the DHA stimuli and the lysosomal inhibitor caused an additive effect, this suggests an increased autophagic turnover of SQSTM1 in response to DHA. Consistently, supplementation with DHA also increased the level of MAP1LC3B-II when combined with lysosomal inhibition (Fig. 1C). This observation indicates an autophagy-inducing activity of DHA in the ARPE-19 cells. To determine the time needed for DHA to induce autophagy and increase the level of SQSTM1, cell extracts were prepared after 3, 6, 16, and 24 h supplementation with DHA and BafA1. Already after 3 h with DHA supplementation, the turnover of both SQSTM1 and MAP1LC3B-II was induced, and the effect lasted for the duration of the experiment (Fig. 1C). The additive effect of DHA supplementation and inhibition of autophagic degradation by BafA1 suggests lipid-induced synthesis of the 2 proteins. In line with this notion, quantitative real-time PCR (qRT-PCR) analyses revealed a more than 7-fold increase in *SQSTM1* mRNA and more than 4-fold increase in *MAP1LC3B* mRNA levels in response to 16 h DHA treatment (Fig. 1D). Interestingly, among the mammalian orthologs of yeast Atg8, the induction of MAP1LC3B seems selective since only minor changes could be detected in mRNA levels of *MAP1LC3A* and *GABARAPL1*. Together, these data suggest that the synthesis of SQSTM1 and MAP1LC3B is induced and autophagy increased in response to DHA in a lipid-specific manner.

Since SQSTM1 was found in the detergent-resistant fraction after DHA supplementation, the cells were immunostained for SQSTM1 and MAP1LC3B. In response to DHA, a transient increase in number and size of SQSTM1-positive punctate cytosolic structures was observed (Fig. 2A). The number of SQSTM1-positive structures increased with time up to 16 h. A partial colocalization with MAP1LC3B was observed, which might represent autophagosomes. To quantify the number of punctate SQSTM1-positive structures per cell, more than 500 cells per condition were analyzed using automated imaging. Consistent with the manual inspection, automated image analyses demonstrated that the average number of SQSTM1 punctate structures increased with time after DHA supplementation (Fig. 2B). The average number of SQSTM1-positive speckles increased from less than 10 per cell in untreated cells to approximately 50 per cell in cells treated with DHA for 16 h.

Interestingly, the number of SQSTM1 speckles that colocalized with MAP1LC3B decreased from approximately 60% in the untreated cells to less than 30% in the cells treated with DHA for 16 h. By extending the treatment time to 24 h, the number of punctate SQSTM1 structures was reduced, and the frequency of colocalization with MAP1LC3B increased (Fig. 2C). Together, these data indicate that cells respond to DHA by inducing a transient increase in SQSTM1-positive speckles. The reduction in the number of these speckles coincides with an increased turnover of MAP1LC3B-II and elevated colocalization between SQSTM1 and MAP1LC3B.

DHA induces a transient increase in ROS and activation of NFE2L2 in ARPE-19 cells

PUFA supplementation causes a rise in the level of reactive oxygen species (ROS) in different cell types,⁵⁶ and to induce oxidative stress response genes in colon cancer cells.⁵⁷ In response to DHA (70 μ M and 140 μ M) there was a significant increase in ROS levels at 3 h and then the level was reduced with time (Fig. 3A). Interestingly, 24 h after adding DHA (140 μ M) the level of ROS was lower compared to control cells. The DHA-induced increase in ROS levels could be counteracted by pre-treating the cells with the exogenous antioxidants N-acetyl-cysteine (NAC) or vitamin E (Fig. 3B). DHA treatment for 3 h resulted in significantly higher levels of ROS compared to treatment with AA or OA for the same time-period (Fig. 3C). Also, no further increase in ROS levels was observed after 6 h and 24 h supplementation with OA or AA (data not shown). Increased levels of ROS represent a stress situation that is counteracted by numerous cellular responses including changes in gene expression coordinated by the transcription factor NFE2L2. In response to ROS, NFE2L2 is stabilized and translocated to the nucleus.⁵⁸ Consistent with the ROS measurements, immunofluorescent analyses demonstrated a clear increase in nuclear localization of NFE2L2 in response to DHA while AA and OA did not affect the level of nuclear NFE2L2 significantly (Fig. 3D). The immunostaining approach for evaluating NFE2L2 activation was specific since *NFE2L2* siRNA caused a loss in intensity (data not shown). In line with a ROS-mediated activation of NFE2L2 after DHA supplementation, pretreatment with NAC counteracted nuclear translocation of NFE2L2 (Fig. 3E) and induction of HMOX1 (heme oxygenase 1) (Fig. 3F), representing one of the typical NFE2L2 targets induced by oxidative stress.⁵⁹ Immunoblot analyses also demonstrated a clear increase in NFE2L2 protein level in response to DHA consistent with a stabilization of the protein (Fig. 3H). Induction of HMOX1 was further analyzed after adding different lipids and found to be selective for DHA (Fig. 3G). Further, induction of NFE2L2 was validated by microarray gene expression analyses Using MetaCore for pathway analyses, it was revealed that NFE2L2-associated stress responses were significantly activated after 12 h DHA treatment ($P < 10^{-6}$). The identified, upregulated NFE2L2 target transcripts included *HMOX1*, *NQO1* (NAD[P]H dehydrogenase, quinone 1), *SRXN1* (sulfiredoxin 1), *ATF4* (activating transcription factor 4), and *SLC7A11* (solute carrier family 7 [anionic amino acid

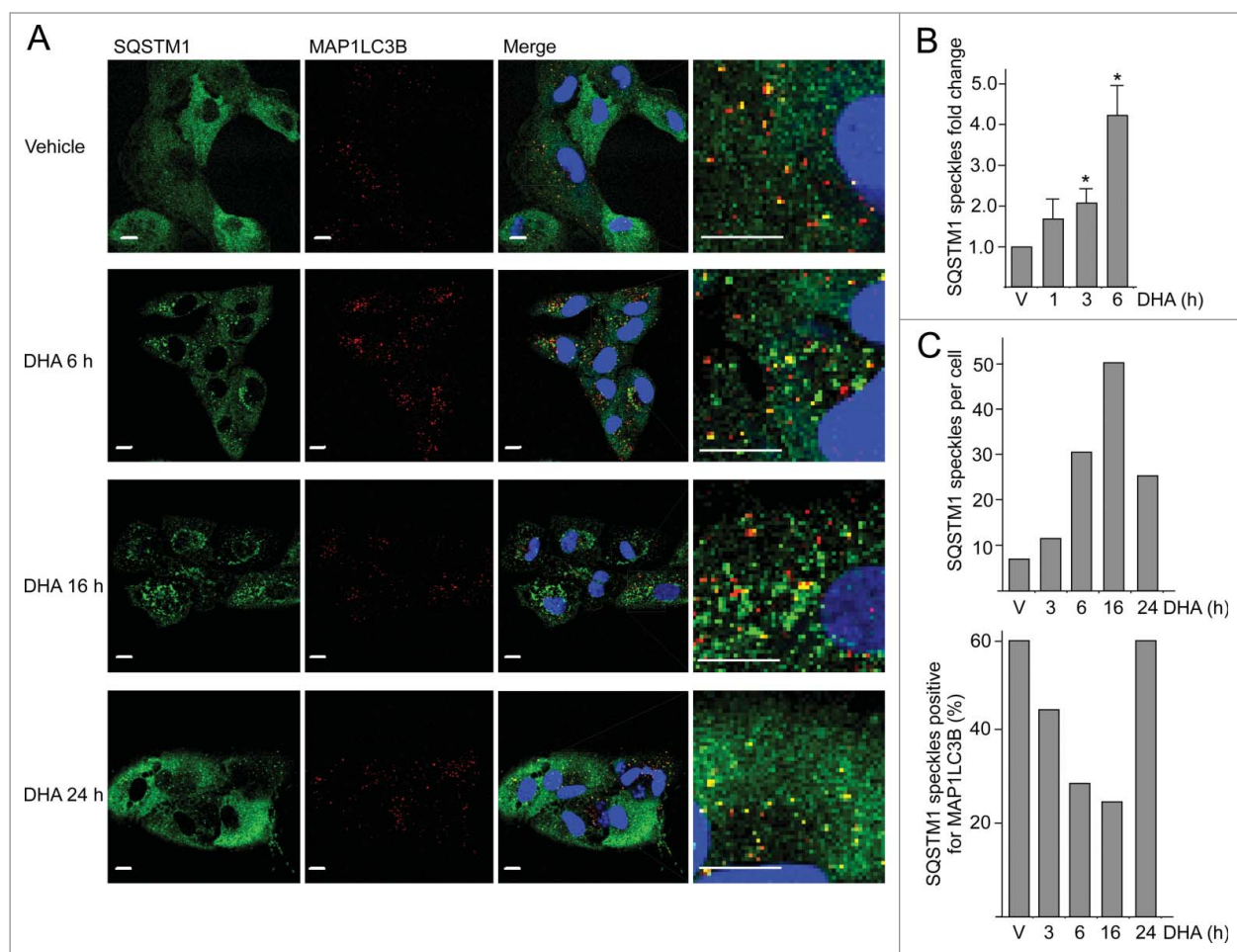


Figure 2. The number of SQSTM1-positive protein speckles in ARPE-19 cells increases after DHA supplementation. **(A)** Immunostaining for SQSTM1 and MAP1LC3B after DHA (70 μ M) treatment for indicated time points. Nuclear DNA was stained using Draq5 (5 μ M). Scale bar: 10 μ m. **(B)** Cells were treated with vehicle (V) or DHA (70 μ M) for 1, 3, and 6 h. The SQSTM1-positive speckles were automatically quantified using ScanR automated image acquisition. The quantification displayed are representative for 3 independent experiments from where 2 are automatically quantified for more than 1,000 cells per condition and one is manually counted. *) indicates significantly different from control, Student *t* test $P < 0.05$. **(C)** The number of SQSTM1-positive speckles per cell (upper panel) and SQSTM1 speckles positive for MAP1LC3B (lower panel) in ARPE-19 cells supplemented with vehicle (V) or DHA (70 μ M) for the indicated time points. The quantification displayed was performed manually for more than 100 cells per condition from one representative experiment. This quantification is representative for 3 independent experiments.

transporter light chain, xc- system], member 11). In line with these findings, the mRNA level of *SQSTM1*, another NFE2L2 target gene, was highly increased after 16 h DHA supplementation determined by qRT-PCR (Fig. 1D). In summary, these data are consistent with a lipid selective induction of ROS that results in elevated transcription of NFE2L2 controlled genes in response to DHA in ARPE-19 cells.

The DHA-induced increase in the protein level of NFE2L2 corresponded with a slight reduction in the protein level of one of its negative regulators KEAP1 (kelch-like ECH-associated protein 1) (Fig. 3H). This reduction was blocked by BafA1, supporting the notion that KEAP1 is degraded by selective autophagy.⁶⁰ Under resting conditions, KEAP1 sequesters NFE2L2 and targets it for proteosomal degradation.⁶¹ Elevated cellular levels of ROS cause KEAP1 to dissociate from

NFE2L2.⁶² In addition, SQSTM1 can sequester KEAP1 and the affinity increases upon phosphorylation of SQSTM1 at serine 351 (Ser351) and this mechanism represents an alternative route to activate NFE2L2.⁶³⁻⁶⁶ Interestingly, using an antibody specific for SQSTM1 phosphorylated at Ser351, a clear raise was observed in response to DHA, but not to AA or OA (Fig. 3I). Inhibition of lysosomal degradation also caused an increase in the cellular level of this modified form of SQSTM1 that was further enhanced by cotreatment with DHA. Together, these data is consistent with DHA-induced ROS and a resulting stabilization and nuclear translocation of NFE2L2. However, we cannot exclude that phosphorylation of SQSTM1 at Ser351 also contributes to the observed activation of NFE2L2. Activation of NFE2L2 results in elevated mRNA and protein levels of SQSTM1 and HMOX1. Prolonged exposure to DHA results in cellular ROS

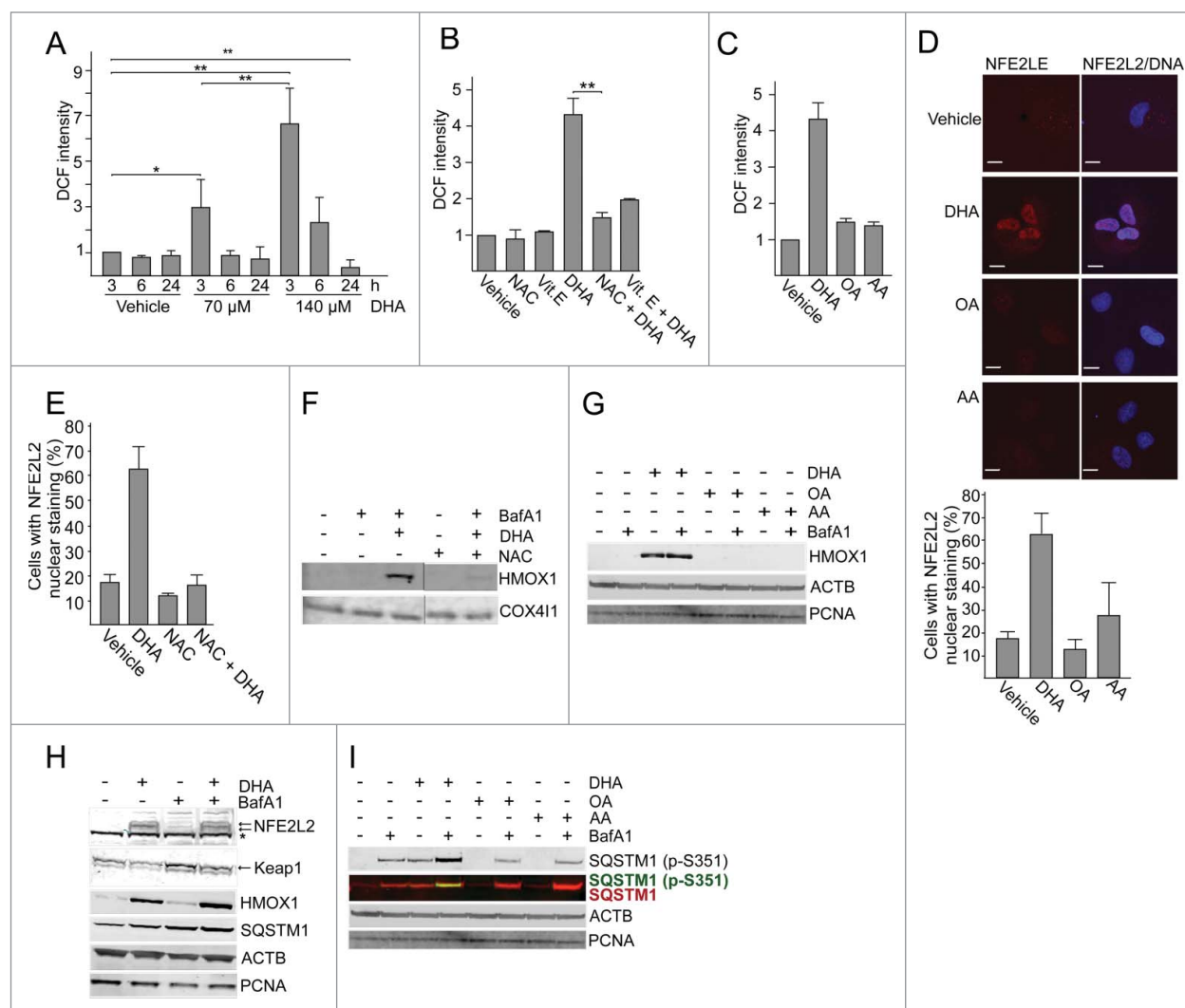


Figure 3. DHA induces a transient increase in ROS and induce NFE2L2 cytoprotective genes. **(A)** Changes in ROS levels measured at different time points after DHA (70 and 140 μM) using a fluorescent ROS DCF probe. The data represent the mean fold change \pm SD for 6 independent experiments for 3 h and 3 independent experiments for 6 h and 24 h. Each experiment was performed in duplicates where the mean intensity of 10,000 cells per well \pm SD was measured. *) indicates significantly different from control, Student *t* test $P < 0.05$ and **) $P < 0.01$. **(B)** Where indicated the cells were pretreated with antioxidants (5 mM N-acetyl-cysteine (NAC) or 150 μM vitamin E) for 16 h before further stimulations with 140 μM DHA for 3 h. The data represent the average of 3 independent experiments for the DHA and NAC treatments and the average of 2 independent experiments for the Vitamin E treatment. Each experiment was performed in duplicates where the mean intensity of 10,000 cells per well \pm SD was measured. **) indicates significantly different from DHA, Student *t* test $P < 0.01$. **(C)** Changes in ROS levels measured 3 h after DHA, OA or AA (140 μM) supplementation using a DCF fluorescent probe. The data represent the average of 3 independent experiments \pm SD for DHA treated samples and 2 independent experiments \pm SD for AA and OA treated samples. Each experiment was performed in duplicates where the mean intensity of 10,000 cells \pm SD per well was measured. **(D)** Immunostaining of NFE2L2 after 70 μM DHA, OA, AA for 6 h. Nuclear DNA was stained using Draq5 (5 μM). Scale bar: 10 μm . The results are representative for 3 independent experiments. Nuclear NFE2L2 staining from one representative experiment was automatically quantified using ScanR automated image acquisition of more than 3,000 cells. Each experiment was performed in duplicates and the data are presented as average percentage number of cells with NFE2L2 nuclear staining \pm SD. **(E)** The cells were pretreated with NAC (5 mM) for 1 h prior to further stimulation with DHA (70 μM) in combination with NAC for 6 h. After fixation, the cells were immunostained for NFE2L2. Data are representative for 2 independent experiments. The percentage of cells with NFE2L2 nuclear staining from one representative experiment was automatically quantified using ScanR automated image acquisition. Each experiment was performed in duplicate and the data displayed represent the average percentage number of cells with NFE2L2 nuclear staining \pm SD. **(F)** ARPE-19 cells were pretreated with NAC (5 mM) for 1 h following stimulation with DHA (70 μM) for 6 h and BafA1 (100 nM) the last 2 h. Levels of HMOX1 was determined by immunoblotting. COX411 was used as loading control. **(G)** The ARPE-19 cells were treated with DHA, OA or AA (70 μM) with or without BafA1 (100 nM) for 16 h before immunoblotting for HMOX1 (100 μg protein loaded). ACTB/ β -actin and PCNA were used as loading controls. **(H)** Immunoblot of NFE2L2, HMOX1, KEAP1 (100 μg protein loaded), SQSTM1, ACTB and PCNA (loaded 20 μg protein) after DHA (70 μM) with or without BafA1 (100 nM) for 16 h. Arrows represent NFE2L2 and KEAP1 bands while *) represents a nonspecific NFE2L2 band. ACTB and PCNA were used as loading controls. **(I)** Cells were treated as in **(G)** and immunoblotted for phosphorylated SQSTM1 (Ser351) and total SQSTM1 (100 μg protein loaded). ACTB and PCNA were used as loading controls. Data shown are representative of 3 or more independent experiments, unless otherwise stated.

levels that are lower compared with control cells indicating an induction of endogenous antioxidants by DHA. Interestingly, pretreating the cells with exogenous antioxidants counteracted the DHA-induced ROS levels as well as nuclear translocation and activation of NFE2L2, indicating that ROS is clearly involved in the DHA-dependent activation of NFE2L2.

NFE2L2, SQSTM1, and ATG5 are important in the cellular responses to DHA by limiting oxidative stress and mediating cell survival

To evaluate the importance of NFE2L2, SQSTM1 and autophagy in the cellular responses toward DHA, the cells were transfected with targeted siRNAs. More than 60% reduction in ATG5 protein level was observed in cells transfected with *ATG5* siRNA. However, the cells with reduced ATG5 protein levels did not display any reduced ability to form MAP1LC3B-II or degrade SQSTM1 (Fig. 4A), indicating that the remaining ATG5 protein provides sufficient catalytic activity to maintain autophagy largely unchanged. This is in line with previous findings reporting that very low levels of ATG12–ATG5 might be sufficient for maintaining autophagy.⁶⁷ Even though no clear reduction in autophagy could be observed in the *ATG5* siRNA transfected cells, we could still observe a tendency of potentiation of ROS levels in response to DHA compared to the control siRNA-transfected cells (Fig. 4B). In addition, downregulation of ATG5 protein levels affected the growth of the cells treated with DHA compared to the control-transfected cells (Fig. 4C). These relative differences in sensitivity toward DHA were also observed by counting the number of viable cells 48 h after adding DHA (data not shown). However, since we were unable to establish a clear reduction in autophagy in the ARPE-19 cells after downregulation of ATG5, we are uncertain how these effects relate to autophagy. We therefore analyzed ROS levels and cell survival after DHA supplementation in wild-type (WT) and *atg5*-deficient mouse embryonic fibroblasts (MEFs). Compared to the WT MEFs, the *atg5*^{-/-} MEFs displayed an elevated basal level of ROS (Fig. 5A) and NFE2L2 (Fig. 5B) in line with previous notions.²⁶ In response to DHA, the level of both ROS and NFE2L2 increased to higher levels in *atg5*^{-/-} MEFs (Fig. 5A and B) and the autophagy-deficient cells were found more sensitive to DHA (Fig. 5C). Together, these findings indicate a cytoprotective role of autophagy in the cellular responses toward DHA.

Using well-established siRNA probes targeting *NFE2L2*,^{28,64} we estimated NFE2L2 to be approximately 70% downregulated by immunostaining (data not shown) and SQSTM1 was reduced more than 50% after cotreatment with DHA and BafA1 (Fig. 6A). Also, the DHA-induced level of HMOX1 was clearly reduced in the *NFE2L2* siRNA-transfected cells compared to the cells transfected with control siRNA (Fig. S2). These results are consistent with an important role of NFE2L2 in the regulation of both HMOX1 and SQSTM1 in response to DHA. The clear reduction in SQSTM1 and HMOX1 indicates an efficient and functional downregulation of NFE2L2. Targeting *SQSTM1* with siRNA caused a more than 90% reduction in the protein level of SQSTM1 (Fig. 6A). Interestingly, the level of MAP1LC3B-I

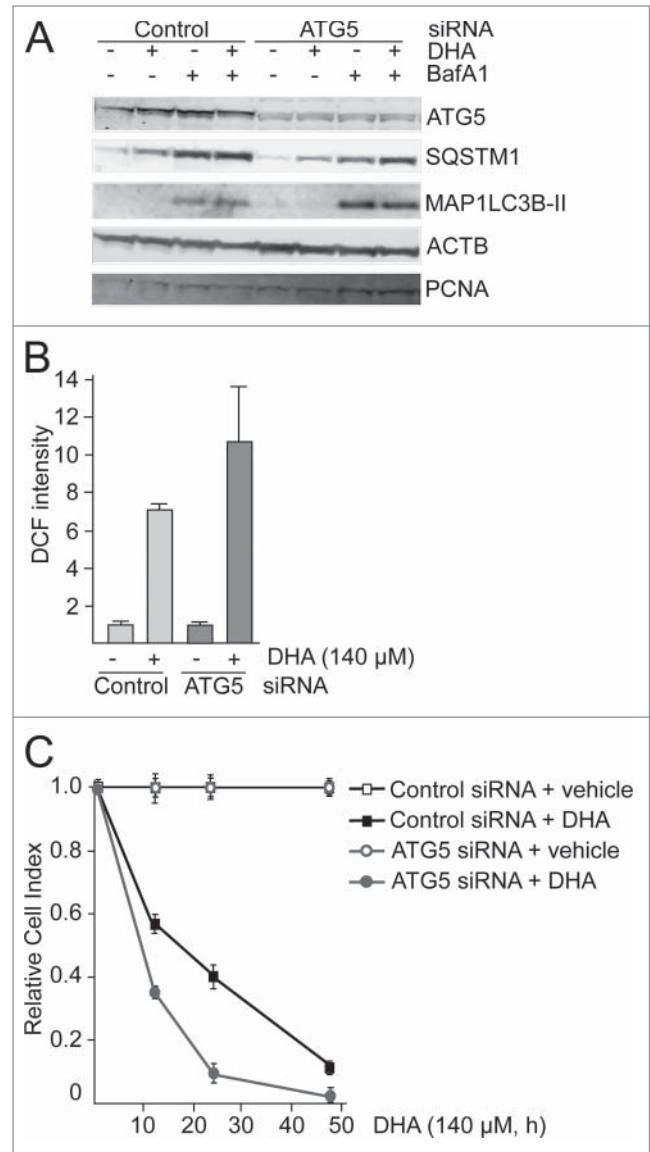


Figure 4. ATG5 is important in the cellular responses to DHA. (A) ARPE-19 cells were transfected with control siRNA or *ATG5* siRNA (100 nM) and left for 24 h before reseeding. Following incubation for 24 h, the cells were added DHA (70 μM) or BafA1 (100 nM) for 24 h and immunoblotted for ATG5, SQSTM1, and MAP1LC3B. ACTB and PCNA were used as loading controls. (B) The cells were siRNA-transfected as in (A). After DHA (140 μM) treatment for 3 h changes in ROS levels were measured using a fluorescent ROS DCF probe. The results are representative for 2 independent experiments. Each experiment was performed in duplicates where the mean intensity ±SD of 10,000 cells per well was measured. The control is normalized to one and the relative fold changes are shown. (C) Relative cell index after transfection with control or *ATG5* siRNA (100 nM) after vehicle or DHA (140 μM) based on real-time monitoring using the xCELLigence instrument. The cell index for each treatment was normalized to one at the start of the experiment. For each time point the cell index of control samples (Control siRNA + vehicle and *ATG5* siRNA + vehicle) was normalized to 1. The effect of DHA treatment after transfection with either Control siRNA or *ATG5* siRNA is shown relative to the corresponding controls. Mean normalized cell index with standard deviation of triplicate wells of vehicle or DHA treated cells is displayed. Data shown are representative for 2 independent experiments.

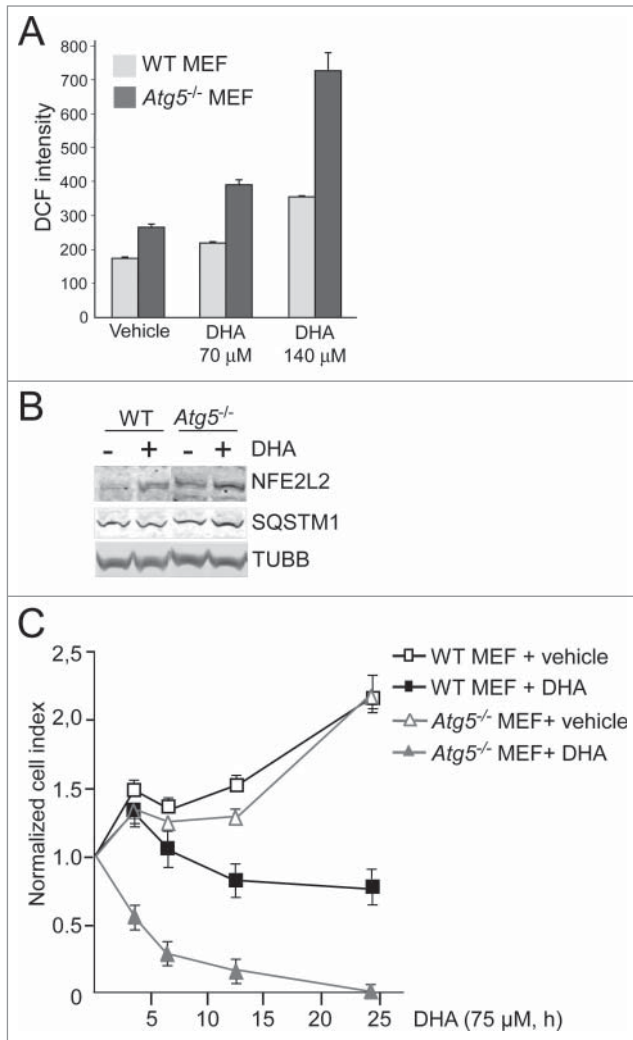


Figure 5. The *atg5* knockout MEFs are more sensitive to DHA compared to wild-type MEFs. **(A)** The levels of ROS were measured in wild-type (WT) and *atg5*^{-/-} MEFs after 3 h DHA treatment (70 and 140 μM) using the fluorescent DCF probe. The data from one representative experiment of 3 independent experiments are displayed. Each experiment was performed in triplicate wells where the mean intensity ±SD of 10,000 cells per well was measured. **(B)** The levels of NFE2L2 and SQSTM1 after vehicle or DHA (70 μM, 16 h) treatment in wild-type and *atg5*^{-/-} MEFs (85 μg protein loaded). TUBB/β-tubulin was used as loading control. The immunoblot is representative for 3 independent experiments. **(C)** Wild-type and *atg5*^{-/-} MEFs were exposed to DHA (75 μM) and cellular responses observed over time using the xCELLigence real-time monitoring system. The cell index was normalized to one at the start of the experiment. Mean normalized cell index ±SD of triplicate wells of vehicle or DHA treated cells are displayed. The results are representative for 5 independent growth experiments scored by cell index using xCELLigence.

was elevated in response to both *NFE2L2* and *SQSTM1* siRNA transfection compared to control siRNA-transfected cells. The induced level of MAP1LC3B-I was evident in the untreated control and further increased in response to DHA, indicating that the cells compensate for reduced levels of NFE2L2 and SQSTM1 by inducing the synthesis of MAP1LC3B protein and activation

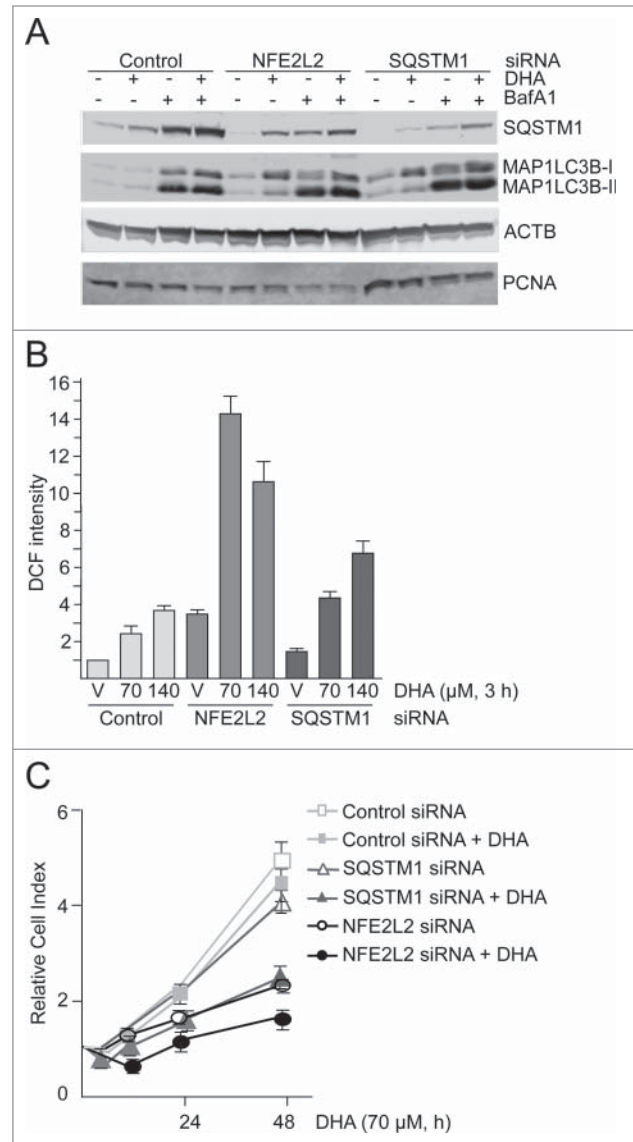


Figure 6. NFE2L2 and SQSTM1 are important in the cellular responses to DHA in ARPE-19 cells. **(A)** Cells were transfected with control, *NFE2L2* and *SQSTM1* siRNA (25 nM) and left for 24 h before reseeding. Following incubation for 24 h, the cells were added DHA (70 μM) or BafA1 (100 nM) for 24 h. Immunoblot for SQSTM1 and MAP1LC3B. ACTB/β-actin and PCNA were used as loading controls. **(B)** The cells were siRNA-transfected as in **(A)**. After vehicle (V) and DHA (70 and 140 μM) treatment for 3 h changes in ROS levels were measured using a fluorescent ROS DCF probe. The data are representative for 2 independent experiments both performed in duplicates. The data represent the mean intensity ±SD of 10,000 cells per well and is displayed as relative DCF intensity. **(C)** Relative cell index after transfection with control, *NFE2L2* or *SQSTM1* siRNA (25 nM) after vehicle and DHA treatment (70 μM) based on real-time monitoring using the xCELLigence instrument. The cell index was normalized to one at the start of the experiment. Mean normalized cell index with standard deviation of triplicate wells of vehicle and DHA treated cells is displayed. Data shown are representative for 3 independent experiments.

of autophagy. Consistent with an important role of NFE2L2 in the cellular responses to DHA, a more than 3-fold increase in

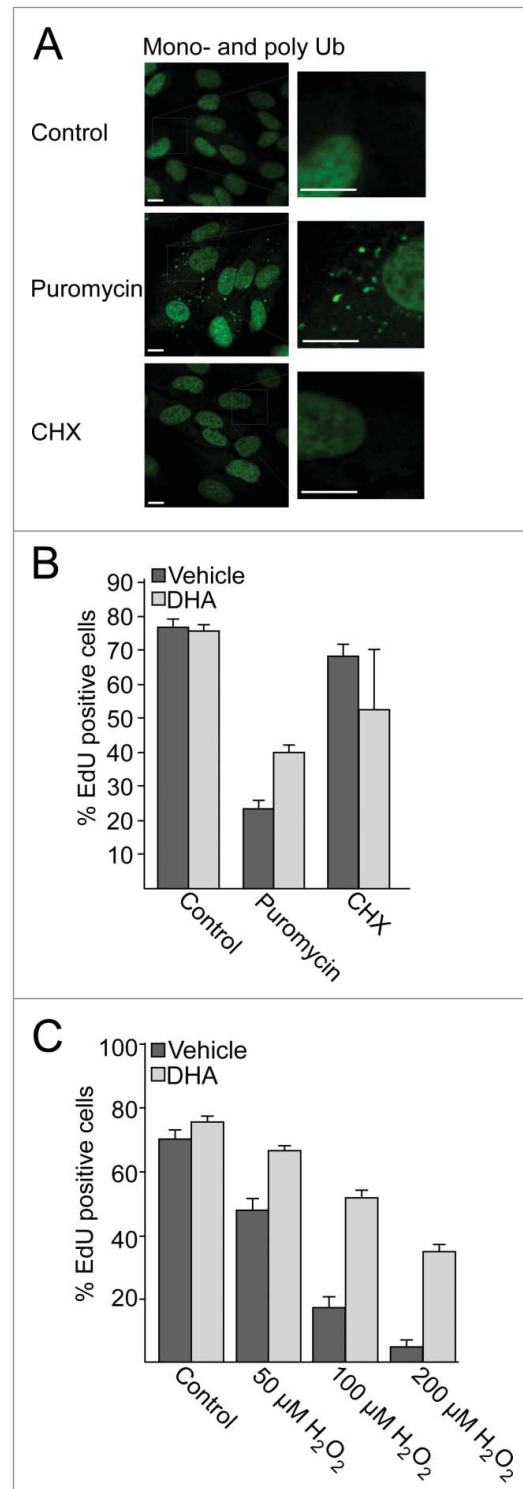
basal ROS levels was observed that was further strongly increased by DHA in the *NFE2L2* siRNA-transfected cells (Fig. 6B). Downregulation of *SQSTM1* also resulted in a slightly increased basal ROS level and a further elevation after DHA supplementation compared to control siRNA-transfected cells. Since *SQSTM1* is only one of a number of different cytoprotective genes controlled by *NFE2L2*, the data demonstrate that downregulation of *NFE2L2* is more severe in terms of basal and induced levels of ROS compared to siRNA-mediated downregulation of *SQSTM1*. Accordingly, real-time monitoring of cells transfected with siRNA against *NFE2L2* and *SQSTM1* displayed a reduced cell growth in the presence of 70 μ M DHA, consistent with a cytostatic effect. Again, siRNA mediated downregulation of *NFE2L2* was found more severe than downregulation of *SQSTM1* after DHA supplementation (Fig. 6C). By increasing DHA concentration (140 μ M), the sensitivity was further increased (data not shown). Together, these results indicate that *NFE2L2*, *SQSTM1* and autophagy cooperate in regulating the cellular responses toward DHA; interfering with any of these processes turns a transient, mild increase in ROS into a cytotoxic stress condition.

DHA mobilizes cytoprotection toward protein aggregates and oxidative stress

Protein aggregates are involved in aging, diseases, and cell death, and autophagic degradation of these aggregates is important for cell survival. We observed that DHA stabilizes and activates *NFE2L2*, and causes a subsequent increase in *SQSTM1* mRNA and protein levels. *SQSTM1* are involved in sequestration of misfolded, ubiquitinated proteins into protein aggregates, and ensures selective degradation of these by autophagy.^{29,68} Therefore, we wanted to investigate if DHA makes the cells more resistant to accumulation of protein aggregates or subsequent oxidative stress. Treating the cells with puromycin, a protein synthesis inhibitor that causes release of premature and misfolded proteins during translation,^{28,69} led to a clear increase in mono- and polyubiquitinated protein aggregates (Fig. 7A). In contrast, no such increase could be observed in response to the translational inhibitor cycloheximide (CHX) for the same period of time.

Figure 7. DHA pretreatment protects ARPE-19 cells against protein aggregates and oxidative stress. (A) Immunostaining for mono- and polyubiquitinated proteins in ARPE-19 cells treated with puromycin (10 μ M) or cycloheximide (CHX, 10 μ g/ml) for 4 h. Scale bar: 10 μ m. (B) The cells were pretreated with vehicle or DHA (70 μ M) for 16 h before stimulation with puromycin (10 μ M) or cycloheximide (CHX, 10 μ g/ml) for 4 h. Following washout and EdU labeling for 16 h the percentage of EdU-positive cells were quantified automatically for more than 3,500 cells using ScanR automated image acquisition. Data shown are representative for 2 independent experiments. (C) After pretreatment with vehicle or DHA for 16 h, the cells were stimulated with hydrogen peroxide (H_2O_2) in the indicated concentrations. After washing and EdU labeling for 16 h the percentage of EdU-positive cells were quantified automatically using ScanR automated image acquisition of more than 3,000 cells. Data shown are representative for 3 independent experiments.

After pretreating the cells with DHA, the cells were further treated with puromycin or cycloheximide for 4 h. The drugs were then removed and the cells were incubated for a further 16 h in the presence of the thymidine analog 5-ethynyl-2'-deoxyuridine (EdU) to evaluate the frequency of cells performing S



phase during this time.⁷⁰ By automated imaging and image analyses of more than 3,500 cells, it was found that more than 75% of the untreated cells displayed nuclei positive for EdU (Fig. 7B). Pretreatment with DHA did not affect the frequency of cells that performed S phase. In response to a 4 h treatment with puromycin, but not cycloheximide, the number of nuclei positive for EdU was clearly reduced compared to control. Interestingly, pretreating the cells with DHA partially rescued the cell proliferation following a puromycin challenge. These results indicate that under conditions where SQSTM1 is induced, there is also an improved tolerance for misfolded proteins formed in response to puromycin.

To test whether activation of NFE2L2 observed after DHA stimulation makes the cells more resistant to subsequent exposure to oxidative stress, ARPE-19 cells were pretreated with DHA for 16 h following a 30 min challenge with hydrogen peroxide (H₂O₂). After washing, cells were incubated for 16 h in the presence of EdU. Again, pretreatment with DHA partially rescued proliferation of the cells (Fig. 7C). Together, these results indicate that DHA induces cellular responses that mobilize resistance to misfolded proteins and oxidative stress.

Discussion

We here demonstrate that the n-3 PUFA DHA selectively induces a transient increase in cellular ROS levels that is counteracted by activation of NFE2L2 and induction of oxidative stress response genes and proteins in ARPE-19 cells. In addition, DHA stimulates the synthesis of SQSTM1 and elevates autophagy. Pretreatment with DHA counteracted cell cycle arrest induced by misfolded proteins or oxidative stress. Together our data indicate that DHA induces an interplay between NFE2L2 activation and autophagy in retinal pigment epithelial cells that makes the cells more tolerant to misfolded proteins and oxidative stress. These responses could represent putative disease preventive mechanisms mobilized after a mild, transient oxidative stress induced by DHA in a lipid selective manner.

Elevated levels of ROS are implicated in the pathogenesis of a number of neurodegenerative diseases, including AMD.^{18,71} NFE2L2 is the main regulator of the expression of genes encoding proteins that controls cellular redox status.^{58,72} Upon aging, *nfe2l2*-knockout mice have an increased risk of developing AMD-like phenotype,⁷³ emphasizing the important cytoprotective role of the cell's endogenous antioxidative system. Physiologically relevant doses of DHA caused a transient increase in ROS followed by increased protein levels and nuclear translocation of NFE2L2. Subsequently, increased expression of NFE2L2-modulated genes was detected by gene-expression arrays, and as increased protein levels of the NFE2L2 regulated proteins HMOX1 and SQSTM1. The n-6 PUFA arachidonic acid and the monounsaturated oleic acid did not cause a similar increase in ROS or activation of NFE2L2. Currently, the mechanisms underlying this lipid selectivity is incompletely understood. However, these lipids serve as precursors for different types of lipid-derived signaling compounds resulting from both

nonenzymatic and enzymatic reactions.⁷⁴ The ARPE-19 cells did not display any changes in cell growth or survival after adding any of the lipids (70 μM). Nevertheless, in cells where NFE2L2 was downregulated, both the basal and DHA-induced levels of ROS were increased consistent with a central role of NFE2L2 in redox balance. Interestingly, in cells depleted for NFE2L2 the growth rate was clearly affected even under normal growth conditions. After DHA supplementation the cytostatic response was further potentiated. These data are consistent with previous reports demonstrating that DHA directly or indirectly induces NFE2L2.^{74,75} Also, we found that DHA pretreatment protected the ARPE-19 cells from a cytostatic effect upon a subsequent challenge with hydrogen peroxide. Together, these results indicate that DHA induces activation of NFE2L2 and an increased buffer capacity for oxidative stress in retinal pigment epithelial cells.

Autophagy has emerged as a cellular process for selective clearance of damaged proteins and organelles, and is crucial to avoid the development of several age-related diseases, including different types of neurodegeneration.⁷⁶⁻⁷⁸ Mice genetically modified to lack autophagy in a tissue-specific manner display early onset neurodegeneration accompanied by accumulation of misfolded protein aggregates and ubiquitinated proteins.^{30,31} Inducible, systemic knockout of autophagy restricts lifespan in mice to 2 to 3 mo due to the development of severe neurodegeneration.³² Interestingly, deletion of *ATG5* in the lens has been reported to result in age-related cataract accompanied by accumulation of polyubiquitinated and oxidized proteins and SQSTM1.⁷⁹ *ATG5* is also required for lysosomal fusion of phagosomes containing photoreceptor outer segments (POS) important in renewal of photoreceptors in RPE cells and thus optimal vision.⁸⁰ Also, it was recently reported that prolonged use of the autophagy inhibitor chloroquine in treatment of malaria, could cause chloroquine-associated visual loss due to degeneration of RPE cells.⁸¹ AMD develops with age and a marked reduction in autophagy activity in the retina of aged mice have been suggested to be involved in age-associated visual loss and retinal dystrophy.⁸² Together, these findings suggest that elevation of autophagy could protect from development of AMD as well as other neurodegenerative diseases. In this context it is interesting that physiologically relevant concentrations of DHA increases autophagy in the ARPE-19 cells. In addition to increased autophagy, we also observed an increased level of *SQSTM1* mRNA and SQSTM1 protein level. SQSTM1 selectively targets misfolded, ubiquitinated proteins for lysosomal degradation by binding both to ubiquitinated cargos, via its UBA domain, and to mammalian orthologs of yeast *Atg8* on the growing phagophore membrane.²⁸ In this way, the elevated levels of SQSTM1 observed after DHA might enhance the cell's capacity to sequester damaged and ubiquitinated proteins into aggregates. In accordance, a transient increase in the number and size of cytosolic protein aggregates positive for SQSTM1 was observed after DHA. The reduction in the number of these speckles coincides with an increased turnover of MAP1LC3B-II and elevated colocalization between SQSTM1 and MAP1LC3B, which may indicate selective removal of these structures by increased autophagy.

Intriguingly, we observe DHA pretreatment to protect ARPE-19 cells from cell cycle arrest induced by misfolded proteins released during protein translation in the presence of puromycin. We speculate that this may be due to DHA-induced increase in SQSTM1 and subsequent aggregation and autophagic clearance. Such a model would be consistent with the protective role of ubiquitination and aggregation of mutant aggregate-prone huntingtin as a mechanism for cell survival,^{22,83} and autophagy as the mechanism responsible for the clearance of these huntingtin aggregates.^{29,84} Also, others have reported that DHA-derived ROS is involved in protein quality control by regulating aggregation and further autophagic degradation of misfolded apolipoprotein B in hepatocytes.⁸⁵

Interestingly, both the basal and DHA-induced level of MAP1LC3B-I were elevated in cells depleted for NFE2L2 and SQSTM1. This increase in MAP1LC3B-I could indicate a compensatory role of autophagy under conditions of increased ROS levels. Downregulation of SQSTM1 did not influence cell growth under normal conditions but resulted in a prominent cytostatic response when combined with DHA treatment. As expected, the cytostatic responses toward DHA after downregulating SQSTM1 were not as clear compared to cells with downregulated NFE2L2. These differential effects likely reflect that NFE2L2 controls a number of mechanisms that counteract oxidative stress where SQSTM1-mediated targeting of misfolded proteins for autophagic degradation is only one of these. The complex interplay between oxidative stress and autophagy is also illustrated by the finding that ROS levels are increased in cancer cells lacking autophagy.⁸⁶ In addition, underscoring the complexity of this interplay, NFE2L2 controls the expression of the autophagy cargo receptor SQSTM1, but at the same time, phosphorylated SQSTM1 partly controls the activity of NFE2L2 by sequestering its negative regulator KEAP1.^{58,64-66} NFE2L2 transcriptionally cooperates with several cellular stress response pathways, including ATF4-regulated stress responses,⁸⁷ that further regulates SQSTM1,⁸⁸ and autophagy.⁸⁹ Also, in addition to TFEB (transcription factor EB),⁹⁰ recent studies have pointed to CREB (cAMP responsive element binding protein) and PPARA (peroxisome proliferator-activated receptor α) important for the transcriptional regulation of autophagy.^{91,92}

The pathogenesis of AMD is strongly associated with oxidative stress.^{10,18,20,93,94} Currently, there is no established prevention or therapy for early AMD. The Age-Related Eye Disease Study (AREDS) is among the largest and most robust randomized clinical trials designed to investigate the role of daily oral supplementation of antioxidant vitamins and minerals.¹³ The AREDS study demonstrated that daily supplementation with antioxidant reduced the risk of developing advanced AMD by 25% at 5 y. Epidemiological studies have suggested a protective role of n-3 PUFAs for developing AMD.^{37-42,95-97} Also, subgroup analysis from the Nutritional AMD Treatment 2 Study from 2013, revealed that high levels of n-3 PUFAs in red blood cells can prevent AMD progression.⁹⁸ To assess if antioxidants and n-3 PUFAs could induce additive effects, a second AREDS2 study was designed to evaluate if inclusion of n-3 PUFAs to the AREDS formulation further reduced the risk of progression to advanced

AMD. However, no additional effect was observed in preventing AMD progression.⁹⁹ Our results demonstrate that DHA potently induces the endogenous oxidative stress defense coordinated by NFE2L2 in ARPE-19 cells. The DHA-induced activation of NFE2L2 was abolished by cotreatment with exogenous antioxidants. Thus, it is possible that the 2 approaches to prevent AMD, either by reducing ROS via exogenous antioxidants, or by n-3 PUFAs to mobilize the endogenous ROS scavenging systems, neutralize each other. Based on our results, it would be interesting to determine if additional effects of the 2 approaches could be present if antioxidants and n-3 PUFAs are sequentially supplemented. However, further research is needed in order to determine the kinetics of the 2 responses in relevant cell types.

Further studies are needed to determine if aggregation, autophagy and NFE2L2 activation are part of the physiological responses to DHA also in vivo. Our data indicate that activation of NFE2L2 and elevated autophagy could represent markers for the disease preventive effects of DHA supplementation. Interestingly, our results emphasize that exogenous antioxidants may interfere with and counteract some of the putative positive effects of DHA, including the activation of NFE2L2. The current study shows that DHA induces the cellular antioxidant responses controlled by NFE2L2 and stimulate protein quality control and autophagy. These cellular mechanisms harbor a number of putative biomarkers that may be utilized in the future to defined and improve disease preventive effects of marine n-3 PUFAs.

Materials and Methods

Cell lines and reagents

ARPE-19 were obtained from ATCC (CRL-2302) and cultured in DMEM:F12 medium (Sigma, D8437), supplemented with fetal bovine serum (10%) (Gibco, 10270-106) and gentamicin (0.05 mg/mL; Gibco, 15710049). Immortalized wild-type (WT) and *atg5*^{-/-} MEFs were a kind gift from Noboru Mizushima and were grown in DMEM (Sigma, D5796) supplemented with fetal bovine serum (10%) (Gibco, 10270-106) and gentamicin (0.05 mg/mL; Gibco, 15710049). All cell lines were maintained in a humidified atmosphere of 5% CO₂; 95% air at 37°C. All experiments were performed in subconfluent, exponentially growing cells that never exceeded passage number 25.

Docosahexaenoic acid (DHA; Cayman, 90310), oleic acid (OA; Cayman, 90260) and arachidonic acid (AA; Cayman, 90010) were added to prewarmed complete medium to the final desired concentration and vortexed at full speed before added to the cells. Vehicle-treated samples were added to the same volumes of absolute ethanol and was used as control throughout all experiments.

Other reagents used: bafilomycin A₁ (BafA1; Sigma, B1793), puromycin (Sigma, P9620), cycloheximide (CHX; Sigma, C4859), and hydrogen peroxide (H₂O₂; Merck Millipore, 108600).

The following antibodies were used: anti-SQSTM1/p62 (Progen, GP62-C); anti-NFE2L2/NRF2 (Santa Cruz Biotechnology, sc-13032); anti-MAP1LC3B/LC3B (Cell Signaling Technology,

D11); anti-HMOX1 (Enzo, ADI-OSA-110), anti-ATG5 (Novus Biologicals, NB110-53818), anti-ACTB/ β -actin (Abcam, ab6276), anti-KEAP1 (Santa Cruz Biotechnology, E20), anti-phospho-SQSTM1/p62 (Ser351; MBL, PM074), anti-mono- and polyubiquitinated conjugates (clone FK2; Biomol, PW8810), anti-TUBB/ β -tubulin (Abcam, ab6046), anti-PCNA (Santa Cruz Biotechnology, sc-7907), anti-COX4I1/COX IV (Abcam, ab33985). All secondary antibodies were from Invitrogen (Alexa conjugates, catalog numbers A-11073, A-21428 and A-11001) or Li-Cor Biotechnology (NIR dye conjugates, catalog numbers 926-32211, 926-32214, 926-32411926-68077, 926-68071, 926-68070).

Microarray gene expression profiling

ARPE-19 cells were treated with vehicle (ethanol) or 70 μ M DHA for 1, 3, 6, 12, and 24 h before RNA isolation using High Pure RNA isolation kit (Roche, 11828665001). Microarray gene expression profiling was performed in independent triplicates for all time points using Illumina HumanHT-12 v4 Expression BeadChip according to the manufacturer's protocol (Illumina). The statistical analysis was based on summary expression measures using the raw data (CEL) files performed by the robust multiarray average method. The statistical analysis was performed in R (<http://www.r-project.org>), using packages Limma from Bioconductor.¹⁰⁰ Differentially expressed genes were selected based on a threshold of 0.05 on the adjusted *P* values. Enrichment analyses was performed in MetaCoreTM (Thomson Reuters, UK) a data-mining and pathway analysis tool. All data have been submitted to ArrayExpress with the accession number E-MTAB-3016.

Quantitative real-time PCR

Total RNA was extracted from DHA treated cells using the High Pure RNA isolation kit. Purity and quantity were measured by Nanodrop. 1 μ g total RNA was used for cDNA synthesis using the iScript Select cDNA synthesis kit (Bio-Rad, 170-8896). The cDNA was diluted 1:10 before real-time PCR was performed in parallel 25 μ l reactions containing 12.5 μ l 2X QuantiTect SYBR Green PCR master mix (Qiagen, 204141) and 2.5 μ l 10X QuantiTect Primer Assay (Qiagen, catalog numbers Hs_SQSTM1_1_SG, Hs_MAP1LC3B_2_SG, Hs_GABARAPL1_1_SG, Hs_MAP1LC3A_1_SG, Hs_GAPDH_2_SG, Hs_ACTB_2_SG). The cycling conditions for the StepOne plus system (Applied Biosystems, Foster City, CA, USA) were 95°C for 15 min, 40 cycles of 94°C for 15 sec, 55°C for 30 sec and 72°C for 30 sec. Relative RNA transcription levels were transformed into linear form by 2^(-deltadeltaCt). Transcripts were normalized to the quantity of *ACTB* for each condition.

siRNA-mediated knockdown

For *NFE2L2* and *SQSTM1* downregulation cells were transfected using 25 nM siRNA oligo (final concentration) by DharmaFECT transfection reagent 1 (Dharmacon, T-2001-03) and compared to 25 nM control nontargeting siRNA. For *ATG5* downregulation cells were transfected using 100 nM siRNA oligos (final concentration) and compared to the same final

concentration of nontargeting siRNA. Following 24 h, the cells were collected by trypsinization and seeded for real-time cell monitoring, ROS measurements and immunoblot analysis. The following smartpool siRNA oligonucleotides were obtained from Dharmacon; control nontargeting siRNA (D-001210-01); *NRF2/NFE2L2* siRNA (D-003755-02), target sequence: 5'-CCAAAGAGCAGUCAAUGA; *SQSTM1* siRNA (J-010230-06) and *ATG5* siRNA (L-004374-00)

Real-time cell monitoring

Real-time growth curves were obtained using an xCELLigence system (Roche) according to the supplier's recommendations in the presence or absence of DHA (70 μ M and 140 μ M). Where indicated, the cells were pretreated with siRNA (nontargeting, *NFE2L2*, *SQSTM1*, or *ATG5*) 24 h before monitoring in real time with or without DHA (70 μ M and 140 μ M).

ScanR automated image acquisition

The microscope-based imaging platform ScanR (Olympus, Hamburg, Germany) were used to image SQSTM1-positive structures in the presence and absence of DHA (70 μ M). Images were taken with a 20 \times objective, using the excitation filters (wavelength [nm]/width [nm]): FITC (485/20) and Draq5 (650/13). For emission, a combination filter (440,521,607 and 700 nm) was used for all fluorophores (Chroma Technology Corp, Bellows Falls, VT). For each well, approximately 2000 cells were counted. The images were analyzed by the ScanR Analysis software (Olympus). Using the ScanR analysis software (Olympus) the number of cells was counted (based on the nuclear-stain) and the number of SQSTM1 dots within the cells (nucleus and surrounding cytosol) or Click EdU-positive nuclei.

Cell proliferation assay

Cell proliferation was monitored using Click-iT[®] EdU Alexa Fluor[®] 488 Imaging Kit (Invitrogen, C10337) according to the manufacturer's protocol. For EdU incorporation experiments, cells were pretreated with vehicle or DHA (70 μ M) for 16 h, washed 2X PBS before further stimulation with puromycin (10 μ M), cycloheximide (10 μ g/ml) for 4h or hydrogen peroxide (50, 100 or 200 μ M) for 30 min. After 2X washing in PBS the cells were added 5-ethynyl-2'-deoxyuridine (EdU) (5 μ M) for 16 h and fixated using 4% paraformaldehyde. For the click reaction the cells were washed in 3% BSA (Sigma, A7906) and permeabilized using 0.5% Triton X-100 (Sigma, T8787) for 20 min. After additional washing the cells were incubated with Click-It reaction cocktail containing Alexa Fluor 488 azide (Invitrogen, C10337) for 30 min. DNA was stained using 5 μ g/ml Hoechst 33342 included in the kit (Invitrogen, C10337). EdU-positive cells were automatically quantified using ScanR automated image acquisition.

Detection of reactive oxygen species

ROS levels were determined using the Image-iT[™] LIVE Green Reactive Oxygen Species Detection Kit (which utilizes 5-(and-6)-carboxy-2',7'-dichlorodihydrofluorescein diacetate [DCF]; Invitrogen, C6827) and a BD FACS Canto flow

cytometer (BD Biosciences, San Jose, CA, USA). The cells were treated with 70 μM or 140 μM of designated lipids for the indicated time points. When indicated, the cells were pretreated for 16 h with 150 μM vitamin E (Sigma, T3251) and 5 mM N-acetyl cysteine (NAC; Sigma, A9165) before DHA treatment (140 μM) for 3 h. The cells were incubated at 37°C and 5% CO₂ with 0.3 μM DCF for 30 min before intracellular ROS was determined. The experiments were performed in duplicates and the data represent mean intensity of 10,000 cells per well \pm SD. The results represent the average of 6 independent experiments for 3 h and 3 independent experiments for 6 and 24 h. For the antioxidant treatments, the results represent the average of 3 and 2 independent experiments for NAC and vitamin E, respectively. For WT and *atg5* knockout MEFs the experiments were performed in triplicates and the data represent the average of 3 independent experiments. *P* values were calculated using the Student *t* test.

Immunostaining

The cell cultures were treated as specified for indicated time points and fixed in 4% paraformaldehyde before immunostaining using indicated antibodies and visualization by fluorescently labeled secondary antibodies. Nuclear DNA was stained using Draq5 (5 μM ; Biostatus, DR50200) or Hoechst 33342. Immunostaining was imaged with an Axiovert200 microscope equipped with a 63 \times 1.2W objective and the confocal module LSM510 META (Carl Zeiss, Jena, Germany). Images were processed using the LSM software and mounted using Canvas 11 (Deneba). Images are representative of more than 200 randomly selected cells in each condition and of 2 or more independent experiments. All images to be compared were taken with the same settings.

Immunoblotting

After the indicated treatment the cells were harvested by trypsinization and lysed in a urea buffer containing 8 M urea (Merck Millipore, 1084870500), 0.5% (v/v) Triton X-100 (Sigma, T8787), 100 mM DTT (Sigma, 646563), Complete[®] protease inhibitor (Roche, 1187350001) and phosphatase inhibitor cocktail II (Sigma, P5726) and III (Sigma, P0044). When indicated, cells were lysed in a buffer containing 0.25% Triton X-100 (Sigma, T8787), 1 % NP40 (Sigma, NP40S), 50 mM Tris-HCl (pH 8.0), 150 mM NaCl, 1 mM EDTA pH 8, Complete[®] protease inhibitor, and phosphatase inhibitor cocktail II (Sigma, P5726) and III (Sigma, P0044). For wild-type and *atg5*^{-/-} MEFs, the extracts for NFE2L2 detection were prepared using a nuclear extract kit (Active

Motif, 11447358). Total protein concentration in the lysates was determined by BioRad protein assay (Bio-Rad, 500-0006). Equal amounts of proteins (20 μg if nothing else stated) were separated using NuPAGE[®] Novex[®] 12% or 4-12% Bis-Tris Gels (Invitrogen). Bound antibodies were imaged by near infrared fluorescence using appropriate fluorescent dye labeled secondary antibodies and an Odyssey Near Infrared scanner (Li-Cor Biosciences, Lincoln, Nebraska, USA). PCNA and COX4I1 were used for normalization purposes. In addition, loading was also detected using immunoblotting for ACTB/ β -actin and TUBB/ β -tubulin. Images were processed using Li-Cor Odyssey software and mounted using the Canvas 11 software (Deneba).

Statistics

Values were expressed as mean \pm standard deviation (SD). Statistical analyses were performed by the 2-tailed Student *t* test, 2-sample assuming equal variances. *P* values < 0.05 was considered statistically significant and is labeled with *) and *P* < 0.01 is labeled with **). Error bars for qRT-PCR represent the standard deviation of triplicate wells.

Disclosure of Potential Conflicts of Interest

No potential conflicts of interest were disclosed.

Acknowledgments

We thank Noboru Mizushima for wild-type and *atg5* knockout MEFs. Arnar Flatberg and Vidar Beisvåg at the Genomics Core Facility (GCF), Faculty of Medicine, NTNU are acknowledged for the support on gene expression profiling. The Cellular and Molecular Imaging Core Facility (CMIC), Faculty of Medicine, NTNU is acknowledged for access to instruments and support.

Funding

This work was supported by grants from the Norwegian Cancer Society and from the Research Council of Norway through its Centres of Excellence funding program, project number 223255/F50.

Supplemental Material

Supplemental data for this article can be accessed on the publisher's website.

References

- Martinez A, Portero-Otin M, Pamplona R, Ferrer I. Protein targets of oxidative damage in human neurodegenerative diseases with abnormal protein aggregates. *Brain Pathol* 2010; 20:281-97; PMID:19725834; <http://dx.doi.org/10.1111/j.1750-3639.2009.00326.x>.
- Sorolla MA, Rodriguez-Colman MJ, Vall-llaura N, Tamarit J, Ros J, Cabisco E. Protein oxidation in Huntington disease. *BioFactors* 2012; 38:173-85; PMID:22473822; <http://dx.doi.org/10.1002/biof.1013>.
- Smith CD, Carney JM, Starke-Reed PE, Oliver CN, Stadtman ER, Floyd RA, Markesbery WR. Excess brain protein oxidation and enzyme dysfunction in normal aging and in Alzheimer disease. *Proc Natl Acad Sci U S A* 1991; 88:10540-3; PMID:1683703; <http://dx.doi.org/10.1073/pnas.88.23.10540>.
- Kuusisto E, Salminen A, Alafuzoff I. Early accumulation of p62 in neurofibrillary tangles in Alzheimer's disease: possible role in tangle formation. *Neuropathol Appl Neurobiol* 2002; 28:228-37; PMID:12060347; <http://dx.doi.org/10.1046/j.1365-2990.2002.00394.x>.
- Zatloukal K, Stumptner C, Fuchsichler A, Heid H, Schnoelzer M, Kenner L, Kleinert R, Prinz M, Aguzzi A, Denk H. p62 Is a common component of cytoplasmic inclusions in protein aggregation diseases. *Am J Pathol* 2002; 160:255-63; PMID:11786419; [http://dx.doi.org/10.1016/S0002-9440\(10\)64369-6](http://dx.doi.org/10.1016/S0002-9440(10)64369-6).
- Nagaoka U, Kim K, Jana NR, Doi H, Maruyama M, Mitsui K, Oyama F, Nukina N. Increased expression

- of p62 in expanded polyglutamine-expressing cells and its association with polyglutamine inclusions. *J Neurochem* 2004; 91:57-68; PMID:15379887; <http://dx.doi.org/10.1111/j.1471-4159.2004.02692.x>.
7. Kaarniranta K, Salminen A, Haapasalo A, Soininen H, Hiltunen M. Age-related macular degeneration (AMD): Alzheimer's disease in the eye? *J Alzheimers Dis* 2011; 24:615-31; PMID:21297256.
 8. Kaarniranta K, Sinha D, Blasiak J, Kauppinen A, Vereb Z, Salminen A, Boulton ME, Petrovski G. Autophagy and heterophagy dysregulation leads to retinal pigment epithelium dysfunction and development of age-related macular degeneration. *Autophagy* 2013; 9:973-84; PMID:23590900; <http://dx.doi.org/10.4161/auto.24546>.
 9. Gehrs KM, Anderson DH, Johnson LV, Hageman GS. Age-related macular degeneration—emerging pathogenetic and therapeutic concepts. *Ann Med* 2006; 38:450-71; PMID:17101537; <http://dx.doi.org/10.1080/07853890600946724>.
 10. Jarrett SG, Boulton ME. Consequences of oxidative stress in age-related macular degeneration. *Mol Aspects Med* 2012; 33:399-417; PMID:22510306; <http://dx.doi.org/10.1016/j.mam.2012.03.009>.
 11. Dorey CK, Wu G, Ebenstein D, Garsd A, Weiter JJ. Cell loss in the aging retina. Relationship to lipofuscin accumulation and macular degeneration. *Invest Ophthalmol Vis Sci* 1989; 30:1691-9; PMID:2759786.
 12. Holz FG, Bellmann C, Margaritidis M, Schutt F, Otto TP, Volcker HE. Patterns of increased in vivo fundus autofluorescence in the junctional zone of geographic atrophy of the retinal pigment epithelium associated with age-related macular degeneration. *Graefes Arch Clin Exp Ophthalmol* 1999; 37:145-52; <http://dx.doi.org/10.1007/s004170050209>.
 13. Age-Related Eye Disease Study Research G. A randomized, placebo-controlled, clinical trial of high-dose supplementation with vitamins C and E, β carotene, and zinc for age-related macular degeneration and vision loss: AREDS report no. 8. *Arch Ophthalmol* 2001; 119:1417-36; PMID:11594942; <http://dx.doi.org/10.1001/archophth.119.10.1417>.
 14. Murdaugh LS, Mandal S, Dill AE, Dillon J, Simon JD, Gaillard ER. Compositional studies of human RPE lipofuscin: mechanisms of molecular modifications. *J Mass Spectrom* 2011; 46:90-5; PMID:21182214; <http://dx.doi.org/10.1002/jms.1865>.
 15. Mullins RF, Russell SR, Anderson DH, Hageman GS. Drusen associated with aging and age-related macular degeneration contain proteins common to extracellular deposits associated with atherosclerosis, elastosis, amyloidosis, and dense deposit disease. *FASEB J* 2000; 14:835-46; PMID:10783137.
 16. Crabb JW, Miyagi M, Gu X, Shadrach K, West KA, Sakaguchi H, Kamei M, Hasan A, Yan L, Rayborn ME, et al. Drusen proteome analysis: an approach to the etiology of age-related macular degeneration. *Proc Natl Acad Sci U S A* 2002; 99:14682-7; PMID:12391305; <http://dx.doi.org/10.1073/pnas.222551899>.
 17. Crabb JW. The proteomics of drusen. *Cold Spring Harb Perspect Med* 2014; 4:a017194; PMID:24799364; <http://dx.doi.org/10.1101/cshperspect.a017194>.
 18. Winkler BS, Boulton ME, Gottsch JD, Sternberg P. Oxidative damage and age-related macular degeneration. *Mol Vis* 1999; 5:32; PMID:10562656.
 19. Kaarniranta K, Salminen A, Eskelinen EL, Kopitz J. Heat shock proteins as gatekeepers of proteolytic pathways—Implications for age-related macular degeneration (AMD). *Ageing Res Rev* 2009; 8:128-39; PMID:19274853; <http://dx.doi.org/10.1016/j.arr.2009.01.001>.
 20. Handa JT. How does the macula protect itself from oxidative stress? *Mol Aspects Med* 2012; 33:418-35; PMID:22503691; <http://dx.doi.org/10.1016/j.mam.2012.03.006>.
 21. Kaganovich D, Kopito R, Frydman J. Misfolded proteins partition between two distinct quality control compartments. *Nature* 2008; 454:1088-95; PMID:18756251; <http://dx.doi.org/10.1038/nature07195>.
 22. Arrasate M, Mitra S, Schweitzer ES, Segal MR, Finkbeiner S. Inclusion body formation reduces levels of mutant huntingtin and the risk of neuronal death. *Nature* 2004; 431:805-10; PMID:15483602; <http://dx.doi.org/10.1038/nature02998>.
 23. Höhn A, König J, Grune T. Protein oxidation in aging and the removal of oxidized proteins. *J Proteomics* 2013; 92:132-59; PMID:23333925; <http://dx.doi.org/10.1016/j.jprot.2013.01.004>.
 24. Xie Z, Klionsky DJ. Autophagosome formation: core machinery and adaptations. *Nat Cell Biol* 2007; 9:1102-9; PMID:17909521; <http://dx.doi.org/10.1038/ncb1007-1102>.
 25. Hoyer-Hansen M, Bastholm L, Szyniarowski P, Campanella M, Szabadkai G, Farkas T, Bianchi K, Fehrenbacher N, Elling F, Rizzuto R, et al. Control of macroautophagy by calcium, calmodulin-dependent kinase kinase- β , and Bcl-2. *Mol Cell* 2007; 25:193-205; PMID:17244528; <http://dx.doi.org/10.1016/j.molcel.2006.12.009>.
 26. Scherz-Shouval R, Shvets E, Fass E, Shorer H, Gil L, Elazar Z. Reactive oxygen species are essential for autophagy and specifically regulate the activity of Atg4. *EMBO J* 2007; 26:1749-60; PMID:17347651; <http://dx.doi.org/10.1038/sj.emboj.7601623>.
 27. Weidberg H, Shvets E, Elazar Z. Biogenesis and cargo selectivity of autophagosomes. *Ann Rev Biochem* 2011; 80:125-56; PMID:21548784; <http://dx.doi.org/10.1146/annurev-biochem-052709-094552>.
 28. Pankiv S, Clausen TH, Lamark T, Brech A, Bruun JA, Outzen H, Overvatn A, Bjorkoy G, Johansen T. p62/SQSTM1 binds directly to Atg8/LC3 to facilitate degradation of ubiquitinated protein aggregates by autophagy. *J Biol Chem* 2007; 282:24131-45; PMID:17580304; <http://dx.doi.org/10.1074/jbc.M702824200>.
 29. Bjorkoy G, Lamark T, Brech A, Outzen H, Perander M, Overvatn A, Stenmark H, Johansen T. p62/SQSTM1 forms protein aggregates degraded by autophagy and has a protective effect on huntingtin-induced cell death. *J Cell Biol* 2005; 171:603-14; PMID:16286508; <http://dx.doi.org/10.1083/jcb.200507002>.
 30. Hara T, Nakamura K, Matsui M, Yamamoto A, Nakahara Y, Suzuki-Migishima R, Yokoyama M, Mishima K, Saito I, Okano H, et al. Suppression of basal autophagy in neural cells causes neurodegenerative disease in mice. *Nature* 2006; 441:885-9; PMID:16625204; <http://dx.doi.org/10.1038/nature04724>.
 31. Komatsu M, Waguri S, Chiba T, Murata S, Iwata J-i, Tanida I, Ueno T, Koike M, Uchiyama Y, Kominami E, et al. Loss of autophagy in the central nervous system causes neurodegeneration in mice. *Nature* 2006; 441:880-4; PMID:16625205; <http://dx.doi.org/10.1038/nature04723>.
 32. Karśli-Uzunbas G, Guo JY, Price S, Teng X, Laddha SV, Khor S, Kalaany NY, Jacks T, Chan CS, Rabinowitz JD, et al. Autophagy is required for glucose homeostasis and lung tumor maintenance. *Cancer Discov* 2014; 4:914-27; PMID:24875857; <http://dx.doi.org/10.1158/2159-8290.CD-14-0363>.
 33. Madeo F, Tavernarakis N, Kroemer G. Can autophagy promote longevity? *Nat Cell Biol* 2010; 12:842-6; PMID:20811357; <http://dx.doi.org/10.1038/ncb0910-842>.
 34. Valapala M, Wilson C, Hose S, Bhutto IA, Grebe R, Dong A, Greenbaum S, Gu L, Sengupta S, Cano M, et al. Lysosomal-mediated waste clearance in retinal pigment epithelial cells is regulated by CRYBA1/betaA3/A1-crystallin via V-ATPase-MTORC1 signaling. *Autophagy* 2014; 10:480-96; PMID:24468901; <http://dx.doi.org/10.4161/auto.27292>.
 35. Weindruch R. The retardation of aging by caloric restriction: studies in rodents and primates. *Toxicol Pathol* 1996; 24:742-5; PMID:8994305; <http://dx.doi.org/10.1177/019262339602400618>.
 36. Rascon B, Hubbard BP, Sinclair DA, Amdam GV. The lifespan extension effects of resveratrol are conserved in the honey bee and may be driven by a mechanism related to caloric restriction. *Aging* 2012; 4:499-508; PMID:22868943.
 37. SanGiovanni JP, Chew EY, Agron E, Clemons TC, Ferris FL, 3rd, Gensler G, Lindblad AS, Milton RC, Seddon JM, Klein R, et al. The relationship of dietary omega-3 long-chain polyunsaturated fatty acid intake with incident age-related macular degeneration: AREDS report no. 23. *Arch Ophthalmol* 2008; 126:1274-9; PMID:18779490; <http://dx.doi.org/10.1001/archophth.126.9.1274>.
 38. Seddon JM, Cote J, Rosner B. Progression of age-related macular degeneration: association with dietary fat, transunsaturated fat, nuts, and fish intake. *Arch Ophthalmol* 2003; 121:1728-37; PMID:14662593; <http://dx.doi.org/10.1001/archophth.121.12.1728>.
 39. Seddon JM, George S, Rosner B. Cigarette smoking, fish consumption, omega-3 fatty acid intake, and associations with age-related macular degeneration: the US Twin Study of Age-Related Macular Degeneration. *Arch Ophthalmol* 2006; 124:995-1001; PMID:16832023; <http://dx.doi.org/10.1001/archophth.124.7.995>.
 40. Chong EW, Kreis AJ, Wong TY, Simpson JA, Guymer RH. Dietary omega-3 fatty acid and fish intake in the primary prevention of age-related macular degeneration: a systematic review and meta-analysis. *Archives of ophthalmology* 2008; 126:826-33; PMID:18541848; <http://dx.doi.org/10.1001/archophth.126.6.826>.
 41. Merle BM, Delyfer MN, Korobelnik JF, Rougier MB, Malet F, Feart C, Le Goff M, Peuchant E, Letenneur L, Dartigues JF, et al. High concentrations of plasma n3 fatty acids are associated with decreased risk for late age-related macular degeneration. *J Nutr* 2013; 143:505-11; PMID:23406618; <http://dx.doi.org/10.3945/jn.112.171033>.
 42. Merle BM, Benlian P, Puche N, Bassols A, Delcourt C, Souied EH, Nutritional AMDTSG. Circulating omega-3 fatty acids and neovascular age-related macular degeneration. *Invest Ophthalmol Visual Sci* 2014; 55:2010-9; PMID:24557349; <http://dx.doi.org/10.1167/iovs.14-13916>.
 43. Serini S, Fasano E, Piccioni E, Cittadini AR, Calviello G. Differential anti-cancer effects of purified EPA and DHA and possible mechanisms involved. *Curr Med Chem* 2011; 18:4065-75; PMID:21824086; <http://dx.doi.org/10.2174/092986711796957310>.
 44. Bazan NG. Cellular and molecular events mediated by docosahexaenoic acid-derived neuroprotectin D1 signaling in photoreceptor cell survival and brain protection. *Prostaglandins Leukot Essent Fatty Acids* 2009; 81:205-11; PMID:19520558; <http://dx.doi.org/10.1016/j.plefa.2009.05.024>.
 45. Dyerberg J. Coronary heart disease in Greenland Inuit: a paradox. Implications for western diet patterns. *Arctic Med Res* 1989; 48:47-54; PMID:2736000.
 46. Friedland RP. Fish consumption and the risk of Alzheimer disease: is it time to make dietary recommendations? *Arch Neurol* 2003; 60:923-4; PMID:12873846; <http://dx.doi.org/10.1001/archneur.60.7.923>.
 47. Caygill CP, Hill MJ. Fish, n-3 fatty acids and human colorectal and breast cancer mortality. *Eur J Cancer Prev* 1995; 4:329-32; PMID:7549825; <http://dx.doi.org/10.1097/00008469-199508000-00008>.
 48. Jing K, Song KS, Shin S, Kim N, Jeong S, Oh HR, Park JH, Seo KS, Heo JY, Han J, et al. Docosahexaenoic acid induces autophagy through p53/AMPK/mTOR signaling and promotes apoptosis in human cancer cells harboring wild-type p53. *Autophagy*

- 2011; 7:1348-58; PMID:21811093; <http://dx.doi.org/10.4161/auto.7.11.16658>.
49. Rovito D, Giordano C, Vizza D, Plastina P, Barone I, Casaburi I, Lanzino M, De Amicis F, Sisci D, Mauro L, et al. Omega-3 PUFA ethanalamides DHEA and EPEA induce autophagy through PPARgamma activation in MCF-7 breast cancer cells. *J Cell Physiol* 2013; 228:1314-22; PMID:23168911; <http://dx.doi.org/10.1002/jcp.24288>.
 50. Shin S, Jing K, Jeong S, Kim N, Song KS, Heo JY, Park JH, Seo KS, Han J, Park JI, et al. The omega-3 polyunsaturated fatty acid DHA induces simultaneous apoptosis and autophagy via mitochondrial ROS-mediated Akt-mTOR signaling in prostate cancer cells expressing mutant p53. *Biomed Res Int* 2013; 2013:568671; PMID:23841076; <http://dx.doi.org/10.1155/2013/568671>.
 51. Williams-Bey Y, Boularan C, Vural A, Huang NN, Hwang IY, Shan-Shi C, Kehrl JH. Omega-3 free fatty acids suppress macrophage inflammasome activation by inhibiting NF-kappaB activation and enhancing autophagy. *PLoS One* 2014; 9:e97957; PMID:24911523; <http://dx.doi.org/10.1371/journal.pone.0097957>.
 52. Hsu HC, Chen CY, Chiang CH, Chen MF. Eicosapentaenoic acid attenuated oxidative stress-induced cardiomyoblast apoptosis by activating adaptive autophagy. *Eur J Nutr* 2014; 53:541-7; PMID:23887854; <http://dx.doi.org/10.1007/s00394-013-0562-2>.
 53. Fukui M, Kang KS, Okada K, Zhu BT. EPA, an omega-3 fatty acid, induces apoptosis in human pancreatic cancer cells: role of ROS accumulation, caspase-8 activation, and autophagy induction. *J Cell Biochem* 2013; 114:192-203; PMID:22903547; <http://dx.doi.org/10.1002/jcb.24354>.
 54. Elvevoll EO, Barstad H, Breimo ES, Brox J, Eilertsen KE, Lund T, Olsen JO, Osterud B. Enhanced incorporation of n-3 fatty acids from fish compared with fish oils. *Lipids* 2006; 41:1109-14; PMID:17269556; <http://dx.doi.org/10.1007/s11745-006-5060-3>.
 55. Dunn KC, Aotaki-Keen AE, Putkey FR, Hjelmeland LM. ARPE-19, a human retinal pigment epithelial cell line with differentiated properties. *Exp Eye Res* 1996; 62:155-69; PMID:8698076; <http://dx.doi.org/10.1006/exer.1996.0020>.
 56. Dai J, Shen J, Pan W, Shen S, Das UN. Effects of polyunsaturated fatty acids on the growth of gastric cancer cells in vitro. *Lipids Health Dis* 2013; 12:71; PMID:23663688; <http://dx.doi.org/10.1186/1476-511X-12-71>.
 57. Jakobsen CH, Storvold GL, Bremseth H, Follestad T, Sand K, Mack M, Olsen KS, Lundemo AG, Iversen JG, Krokan HE, et al. DHA induces ER stress and growth arrest in human colon cancer cells: associations with cholesterol and calcium homeostasis. *J Lipid Res* 2008; 49:2089-100; PMID:18566476; <http://dx.doi.org/10.1194/jlr.M700389.JLR200>.
 58. Hayes JD, Dinkova-Kostova AT. The Nrf2 regulatory network provides an interface between redox and intermediary metabolism. *Trends Biochem Sci* 2014; 39:199-218; PMID:24647116; <http://dx.doi.org/10.1016/j.tibs.2014.02.002>.
 59. Anwar AA, Li FY, Leake DS, Ishii T, Mann GE, Siow RC. Induction of heme oxygenase 1 by moderately oxidized low-density lipoproteins in human vascular smooth muscle cells: role of mitogen-activated protein kinases and Nrf2. *Free Radic Biol Med* 2005; 39:227-36; PMID:15964514; <http://dx.doi.org/10.1016/j.freeradbiomed.2005.03.012>.
 60. Taguchi K, Fujikawa N, Komatsu M, Ishii T, Unno M, Akaike T, Motohashi H, Yamamoto M. Keap1 degradation by autophagy for the maintenance of redox homeostasis. *Proc Natl Acad Sci U S A* 2012; 109:13561-6; PMID:22872865; <http://dx.doi.org/10.1073/pnas.1121572109>.
 61. Kobayashi A, Kang MI, Okawa H, Ohtsuiji M, Zenke Y, Chiba T, Igarashi K, Yamamoto M. Oxidative stress sensor Keap1 functions as an adaptor for Cul3-based E3 ligase to regulate proteasomal degradation of Nrf2. *Mol Cell Biol* 2004; 24:7130-9; PMID:15282312; <http://dx.doi.org/10.1128/MCB.24.16.7130-7139.2004>.
 62. Itoh K, Wakabayashi N, Katoh Y, Ishii T, Igarashi K, Engel JD, Yamamoto M. Keap1 represses nuclear activation of antioxidant responsive elements by Nrf2 through binding to the amino-terminal Neh2 domain. *Genes Dev* 1999; 13:76-86; PMID:9887101; <http://dx.doi.org/10.1101/gad.13.1.76>.
 63. Lau A, Wang XJ, Zhao F, Villeneuve NF, Wu T, Jiang T, Sun Z, White E, Zhang DD. A noncanonical mechanism of Nrf2 activation by autophagy deficiency: direct interaction between Keap1 and p62. *Mol Cell Biol* 2010; 30:3275-85; PMID:20421418; <http://dx.doi.org/10.1128/MCB.00248-10>.
 64. Jain A, Lamark T, Sjøttem E, Larsen KB, Awuh JA, Overvatn A, McMahon M, Hayes JD, Johansen T. p62/SQSTM1 is a target gene for transcription factor NRF2 and creates a positive feedback loop by inducing antioxidant response element-driven gene transcription. *J Biol Chem* 2010; 285:22576-91; PMID:20452972; <http://dx.doi.org/10.1074/jbc.M110.118976>.
 65. Komatsu M, Kurokawa H, Waguri S, Taguchi K, Kobayashi A, Ichimura Y, Sou YS, Ueno I, Sakamoto A, Tong KI, et al. The selective autophagy substrate p62 activates the stress responsive transcription factor Nrf2 through inactivation of Keap1. *Nat Cell Biol* 2010; 12:213-23; PMID:20173742.
 66. Ichimura Y, Waguri S, Sou Y-s, Kageyama S, Hasegawa J, Ishimura R, Saito T, Yang Y, Kouno T, Fukutomi T, et al. Phosphorylation of p62 Activates the Keap1-Nrf2 Pathway during Selective Autophagy. *Mol Cell* 2013; 51:618-31; PMID:24011591; <http://dx.doi.org/10.1016/j.molcel.2013.08.003>.
 67. Hosokawa N, Hara Y, Mizushima N. Generation of cell lines with tetracycline-regulated autophagy and a role for autophagy in controlling cell size. *FEBS Lett* 2006; 580:2623-9; PMID:16647067; <http://dx.doi.org/10.1016/j.febslet.2006.04.008>.
 68. Rogov V, Dotsch V, Johansen T, Kirkin V. Interactions between autophagy receptors and ubiquitin-like proteins form the molecular basis for selective autophagy. *Mol Cell* 2014; 53:167-78; PMID:24462201; <http://dx.doi.org/10.1016/j.molcel.2013.12.014>.
 69. Szeto J, Kaniuk NA, Canadien V, Nisman R, Mizushima N, Yoshimori T, Bazzett-Jones DP, Brumell JH. ALIS are stress-induced protein storage compartments for substrates of the proteasome and autophagy. *Autophagy* 2006; 2:189-99; PMID:16874109; <http://dx.doi.org/10.4161/auto.2731>.
 70. Asano M, Yamamoto T, Tsuruta T, Nishimura N, Sonoyama K. Dual labeling with 5-bromo-2'-deoxyuridine and 5-ethynyl-2'-deoxyuridine for estimation of cell migration rate in the small intestinal epithelium. *Dev Growth Differ* 2014; 57(1):68-73.
 71. Uttara B, Singh AV, Zamboni P, Mahajan RT. Oxidative stress and neurodegenerative diseases: a review of upstream and downstream antioxidant therapeutic options. *Curr Neuropharmacol* 2009; 7:65-74; PMID:19721819; <http://dx.doi.org/10.2174/157015909787602823>.
 72. Sporn MB, Liby KT. NRF2 and cancer: the good, the bad and the importance of context. *Nat Rev Cancer* 2012; 12:564-71; PMID:22810811; <http://dx.doi.org/10.1038/nrc3278>.
 73. Zhao Z, Chen Y, Wang J, Sternberg P, Freeman ML, Grossniklaus HE, Cai J. Age-related retinopathy in NRF2-deficient mice. *PLoS One* 2011; 6:e19456; PMID:21559389; <http://dx.doi.org/10.1371/journal.pone.0019456>.
 74. Gao L, Wang J, Sekhar KR, Yin H, Yared NF, Schneider SN, Sasi S, Dalton TP, Anderson ME, Chan JY, et al. Novel n-3 fatty acid oxidation products activate Nrf2 by destabilizing the association between Keap1 and Cullin3. *J Biol Chem* 2007; 282:2529-37; PMID:17127771; <http://dx.doi.org/10.1074/jbc.M607622200>.
 75. Cipollina C, Salvatore SR, Muldoon MF, Freeman BA, Schopfer FJ. Generation and dietary modulation of anti-inflammatory electrophilic omega-3 fatty acid derivatives. *PLoS One* 2014; 9:e94836; PMID:24736647; <http://dx.doi.org/10.1371/journal.pone.0094836>.
 76. Levine B, Kroemer G. Autophagy in the pathogenesis of disease. *Cell* 2008; 132:27-42; PMID:18191218; <http://dx.doi.org/10.1016/j.cell.2007.12.018>.
 77. Levine B, Kroemer G. Autophagy in aging, disease and death: the true identity of a cell death impostor. *Cell Death Differ* 2009; 16:1-2; PMID:19079285; <http://dx.doi.org/10.1038/cdd.2008.139>.
 78. Rubinsztein DC. The roles of intracellular protein-degradation pathways in neurodegeneration. *Nature* 2006; 443:780-6; PMID:17051204; <http://dx.doi.org/10.1038/nature05291>.
 79. Morishita H, Eguchi S, Kimura H, Sasaki J, Sakamaki Y, Robinson ML, Sasaki T, Mizushima N. Deletion of autophagy-related 5 (Atg5) and Pik3c3 genes in the lens causes cataract independent of programmed organelle degradation. *J Biol Chem* 2013; 288:11436-47; PMID:23479732; <http://dx.doi.org/10.1074/jbc.M112.437103>.
 80. Kim JY, Zhao H, Martinez J, Doggett TA, Kolesnik AV, Tang PH, Ablonczy Z, Chan CC, Zhou Z, Green DR, et al. Noncanonical autophagy promotes the visual cycle. *Cell* 2013; 154:365-76; PMID:23870125; <http://dx.doi.org/10.1016/j.cell.2013.06.012>.
 81. Bae EJ, Kim KR, Tsang SH, Park SP, Chang S. Retinal damage in chloroquine maculopathy, revealed by high resolution imaging: a case report utilizing adaptive optics scanning laser ophthalmoscopy. *Korean J Ophthalmol* 2014; 28:100-7; PMID:24505207; <http://dx.doi.org/10.3341/kjo.2014.28.1.100>.
 82. Rodriguez-Muela N, Koga H, Garcia-Ledo L, de la Villa P, de la Rosa EJ, Cuervo AM, Boya P. Balance between autophagic pathways preserves retinal homeostasis. *Aging cell* 2013; 12:478-88; PMID:23521856; <http://dx.doi.org/10.1111/acel.12072>.
 83. Steffan JS, Agrawal N, Pallos J, Rockabrand E, Trotman LC, Slepko N, Illes K, Lukacsovich T, Zhu YZ, Cattaneo E, et al. SUMO modification of Huntingtin and Huntington's disease pathology. *Science* 2004; 304:100-4; PMID:15064418; <http://dx.doi.org/10.1126/science.1092194>.
 84. Ravikumar B, Duden R, Rubinsztein DC. Aggregate-prone proteins with polyglutamine and polyalanine expansions are degraded by autophagy. *Hum Mol Genet* 2002; 11:1107-17; PMID:11978769; <http://dx.doi.org/10.1093/hmg/11.9.1107>.
 85. Pan M, Maitin V, Parathath S, Andreu U, Lin SX, St Germain C, Yao Z, Maxfield FR, Williams KJ, Fisher EA. Presecretory oxidation, aggregation, and autophagic destruction of apoprotein-B: a pathway for late-stage quality control. *Proc Natl Acad Sci U S A* 2008; 105:5862-7; PMID:18391222; <http://dx.doi.org/10.1073/pnas.0707460104>.
 86. Mathew R, Karp CM, Beaudoin B, Vuong N, Chen G, Chen HY, Bray K, Reddy A, Bhanot G, Gelinas C, et al. Autophagy suppresses tumorigenesis through elimination of p62. *Cell* 2009; 137:1062-75; PMID:19524509; <http://dx.doi.org/10.1016/j.cell.2009.03.048>.
 87. Miyamoto N, Izumi H, Miyamoto R, Bin H, Kondo H, Tawara A, Sasaguri Y, Kohno K. Transcriptional regulation of activating transcription factor 4 under oxidative stress in retinal pigment epithelial ARPE-19/HPV-16 cells. *Invest Ophthalmol Vis Sci* 2011; 52:1226-34; PMID:21087962; <http://dx.doi.org/10.1167/iov.10-5775>.
 88. B'Chir W, Maurin AC, Carraro V, Averous J, Jousse C, Muranishi Y, Parry L, Stepien G, Fafournoux P,

- Bruhat A. The eIF2alpha/ATF4 pathway is essential for stress-induced autophagy gene expression. *Nucleic Acids Res* 2013; 41:7683-99; PMID:23804767; <http://dx.doi.org/10.1093/nar/gkt563>.
89. Rzymiski T, Milani M, Pike L, Buffa F, Mellor HR, Winchester L, Pires I, Hammond E, Ragoussis I, Harris AL. Regulation of autophagy by ATF4 in response to severe hypoxia. *Oncogene* 2010; 29:4424-35; PMID:20514020; <http://dx.doi.org/10.1038/onc.2010.191>.
 90. Settembre C, Di Malta C, Polito VA, Garcia Arencibia M, Vetrini F, Erdin S, Erdin SU, Huynh T, Medina D, Colella P, et al. TFEB links autophagy to lysosomal biogenesis. *Science* 2011; 332:1429-33; PMID:21617040; <http://dx.doi.org/10.1126/science.1204592>.
 91. Seok S, Fu T, Choi SE, Li Y, Zhu R, Kumar S, Sun X, Yoon G, Kang Y, Zhong W, et al. Transcriptional regulation of autophagy by an FXR-CREB axis. *Nature* 2014; 516:108-11; PMID:25383523.
 92. Lee JM, Wagner M, Xiao R, Kim KH, Feng D, Lazar MA, Moore DD. Nutrient-sensing nuclear receptors coordinate autophagy. *Nature* 2014; 516:112-5; PMID:25383539.
 93. Kinnunen K, Petrovski G, Moe MC, Berta A, Kaarniranta K. Molecular mechanisms of retinal pigment epithelium damage and development of age-related macular degeneration. *Acta Ophthalmol* 2012; 90:299-309; PMID:22112056; <http://dx.doi.org/10.1111/j.1755-3768.2011.02179.x>.
 94. Bhutto I, Luty G. Understanding age-related macular degeneration (AMD): relationships between the photoreceptor/retinal pigment epithelium/Bruch's membrane/choriocapillaris complex. *Mol Aspects Med* 2012; 33:295-317; PMID:22542780; <http://dx.doi.org/10.1016/j.mam.2012.04.005>.
 95. Chong EW, Robman LD, Simpson JA, Hodge AM, Aung KZ, Dolphin TK, English DR, Giles GG, Guymer RH. Fat consumption and its association with age-related macular degeneration. *Arch Ophthalmol* 2009; 127:674-80; PMID:19433719; <http://dx.doi.org/10.1001/archophthalmol.2009.60>.
 96. Christen WG, Schaumberg DA, Glynn RJ, Buring JE. Dietary omega-3 fatty acid and fish intake and incident age-related macular degeneration in women. *Arch Ophthalmol* 2011; 129:921-9; PMID:21402976; <http://dx.doi.org/10.1001/archophthalmol.2011.34>.
 97. Tan JS, Wang JJ, Flood V, Mitchell P. Dietary fatty acids and the 10-year incidence of age-related macular degeneration: the Blue Mountains Eye Study. *Arch Ophthalmol* 2009; 127:656-65; PMID:19433717; <http://dx.doi.org/10.1001/archophthalmol.2009.76>.
 98. Souied EH, Delcourt C, Querques G, Bassols A, Merle B, Zourani A, Smith T, Benlian P. Nutritional AMDTSG. Oral docosahexaenoic acid in the prevention of exudative age-related macular degeneration: the Nutritional AMD Treatment 2 study. *Ophthalmology* 2013; 120:1619-31; PMID:23395546; <http://dx.doi.org/10.1016/j.ophtha.2013.01.005>.
 99. Age-Related Eye Disease Study 2 Research G. Lutein + zeaxanthin and omega-3 fatty acids for age-related macular degeneration: the Age-Related Eye Disease Study 2 (AREDS2) randomized clinical trial. *Jama* 2013; 309:2005-15; PMID:23644932; <http://dx.doi.org/10.1001/jama.2013.4997>.
 100. Gentleman RC, Carey VJ, Bates DM, Bolstad B, Dettling M, Dudoit S, Ellis B, Gautier L, Ge Y, Gentry J, et al. Bioconductor: open software development for computational biology and bioinformatics. *Genome Biol* 2004; 5:R80; PMID:15461798; <http://dx.doi.org/10.1186/gb-2004-5-10-r80>.